chemistry

MDPI

Article

Monofluorophosphates—New Examples and a Survey of the PO_3F^{2-} Anion

Matthias Weil

Institute for Chemical Technologies and Analytics, Division of Structural Chemistry, TU Wien,
Getreidemarkt 9/164-SC, A-1060 Vienna, Austria; Matthias.Weil@tuwien.ac.at

Abstract: During a systematic study of monofluorophosphates, i.e., compounds comprising the tetrahedral anion PO_3F^{2-}, twelve, for the most part new, compounds were obtained from aqueous solutions. Crystal structure refinements based on single crystal X-ray diffraction data revealed the previously unknown crystal structures of $CdPO_3F(H_2O)_2$, $Cr_2(PO_3F)_3(H_2O)_{18.8}$, $Pb_2(PO_3F)Cl_2(H_2O)$, $(NH_4)_2M(PO_3F)_2(H_2O)_2$ (M = Mg, Mn, Co), $NH_4Cr(PO_3F)_2(H_2O)_6$, $NH_4Cu_2(H_3O_2)(PO_3F)_2$, $(NH_4)_2Zn(PO_3F)_2(H_2O)_{0.2}$, and $(NH_4)_2Zn_3(PO_3F)_4(H_2O)$, as well as redeterminations of $ZnPO_3F(H_2O)_{2.5}$ and $(NH_4)_2Ni(PO_3F)_2(H_2O)_6$. From the previously unknown crystal structures, $CdPO_3F(H_2O)_2$ (space group $P\bar{1}$), $Cr_2(PO_3F)_3(H_2O)_{18.8}$ ($P\bar{1}$), $Pb_2(PO_3F)Cl_2(H_2O)$ ($Pnma$), $NH_4Cr(PO_3F)_2(H_2O)_6$ ($R\bar{3}m$), $(NH_4)_2Zn(PO_3F)_2(H_2O)_{0.2}$ ($C2/c$), and $(NH_4)_2Zn_3(PO_3F)_4(H_2O)$ ($I\bar{4}3d$) each crystallizes in an unique crystal structure, whereas compounds $(NH_4)_2M(PO_3F)_2(H_2O)_2$ (M = Mg, Co) crystallize in the $(NH_4)_2Cu(PO_3F)_2(H_2O)_2$ type of structure ($C2/m$) and $(NH_4)_2Mn(PO_3F)_2(H_2O)_2$ in a subgroup thereof ($P2_1/n$, with a klassengleiche relationship of index 2), and $NH_4Cu_2(H_3O_2)(PO_3F)_2$ ($C2/m$) crystallizes isotypically with natrochalcite-type $KCu_2(H_3O_2)(SO_4)_2$. A survey on the PO_3F^{2-} anion, including database entries of all inorganic compounds comprising this group, revealed mean bond lengths of P–O = 1.506(13) Å, P–F = 1.578(20) Å, and angles of O–P–O = 113.7(1.7)° and O–P–F = 104.8(1.7)°, using a dataset of 88 independent PO_3F^{2-} anions or entities. For those crystal structures of monofluorophosphates where hydrogen bonding is present, in the vast majority of cases, hydrogen bonds of the type D–H···F–P (D = O, N) are not developed.

Keywords: monofluorophosphate; crystal growth; mean bond lengths and angles; structure determination; relationship monofluorophosphate and sulfate; D–H···F hydrogen bonds

check for updates

Citation: Weil, M. Monofluorophosphates—New Examples and a Survey of the PO_3F^{2-} Anion. *Chemistry* **2021**, *3*, 45–73. https://doi.org/10.3390/chemistry3010005

Received: 14 December 2020
Accepted: 1 January 2021
Published: 7 January 2021

1. Introduction

The family of monofluorophosphates comprising the PO_3F^{2-} anion was introduced by Lange more than 90 years ago [1]. In the PO_3F^{2-} anion, the fluorine atom is directly bound to the phosphorus atom. However, in the literature, compounds with discrete PO_4^{3-} and F^- anions are also sometimes incorrectly described as "fluorophosphates", e.g., Mn_2PO_4F [2] or Na_2FePO_4F [3]. These compounds correctly belong to the family of 'phosphate fluorides'. Various preparation methods for monofluorophosphates as well as applications of this family of compounds as additives in toothpastes, wood preservatives, corrosion inhibitors, solubility inhibitors for lead in potable water sources, or as active agents against osteoporosis or caries during biomineralization of fluoroapatite were summarized some time ago [4]. More recently, some monofluorophosphates were also shown to exhibit excellent nonlinear optical (NLO) behaviour [5].

In his seminal paper, Lange emphasized the chemical relationships between monofluorophosphates and sulfates in terms of solubilities and reaction behaviours. In fact, the PO_3F^{2-} anion is isoelectronic with the SO_4^{2-} anion, and both anions have a tetrahedral shape, as later evidenced by the very first structure determination of a monofluorophosphate [6]. Prior to this first experimental proof about the structure and shape of the PO_3F^{2-} anion, it was assumed that monofluorophosphates are *isomorphic* with corresponding sulfates [7]. It should be noted that also the terms *isomorphic/isomorphism* still are found in literature to express structural relationships, but their use is not recommended any longer [8]. More appropriate terms are *isostructural/isostructurality* or synonymous *isotypic/isotypism*. Meanwhile, numerous other monofluorophosphates were synthesized and structurally determined, but not for all reported monofluorophosphates corresponding sulfates even exist or show isotypism with existing sulfates.

The current study was undertaken to add more examples of structurally determined monofluorophosphates with inorganic cations to the already existing list of this family of compounds. Although some of the monofluorophosphates investigated during this study have previously been reported and their powder diffraction data deposited in the International Centre for Diffraction Data's (ICDD) powder diffraction file (PDF) [9], structural details of corresponding phases are still missing up to now. As it turned out, some of the data compiled in the PDF at that time are incorrect (wrong space groups, wrong unit cell volume) and were revised during the current study. Moreover, results of the present crystal structure analyses were used under special emphasis to review structural characteristics (bond lengths and angles, point group symmetries) and hydrogen-bonding features of the PO_3F^{2-} anions as well as their structural relationships to corresponding sulfates. O and F atoms differ only in one electron and thus have very similar atomic form factors for X-rays. Consequently, a distinction of the two atom types on the basis of X-ray diffraction methods alone is not free from ambiguity, as was recently shown for minerals that were claimed to comprise monofluorophosphate groups [10]. Nevertheless, the result of the current structure evaluation for the PO_3F^{2-} anion is a useful tool to correctly assign F and O atoms in monofluorophosphates, as exemplified by using structure data of a published crystal structure with incorrectly assigned F and O atoms.

2. Materials and Methods

2.1. Syntheses and Single Crystal Growth

For syntheses of NH_4^+-containing monofluorophosphates, the starting compound $(NH_4)_2PO_3F(H_2O)$ was prepared according to Schülke and Kayser [11] and its purity checked with X-ray powder diffraction (XRPD). One gram of this material was dissolved in 10 mL of a methanol/water mixture (1:1 *v*:*v*). Then, 80 mg solid $AgNO_3$ were added to this solution to precipitate the phosphate anions present due to incomplete conversion or partial hydrolysis of the PO_3F^{2-} anion. The yellow Ag_3PO_4 was filtered off, and the filtrate was repeatedly checked for PO_4^{3-} anions by adding a few drops of an $AgNO_3$ solution until no more clouding was observed in the filtrate, ensuring that all PO_4^{3-} anions were removed. Then, 10 mL of a solution consisting of 500 mg of the respective metal chloride in methanol/water (1:1 *v*:*v*) were added to the monofluorophosphate solution. The excessive Ag^+ ions were precipitated as AgCl and filtered off. To the remaining clear filtrate 100 mL of an acetone/methanol solution (2:1 *v*:*v*) were slowly added, resulting in flocculent precipitates in all cases. The respective suspensions were stirred for one hour and then were filtered. The obtained solids were washed with methanol and acetone and then dried in an exsiccator overnight. XRPD revealed an amorphous state for the obtained materials, except for $(NH_4)_2Mg(PO_3F)_2(H_2O)_2$ that was obtained as a pure polycrystalline phase (cf. PDF entry #00-059-0045).

For single crystal growth of NH_4^+-containing monofluorophosphates, 100 mg of the as-precipitated solids were dissolved in 10 mL of a methanol/water mixture (1:1 *v*:*v*), to some extent under mild warming. The clear solutions were allowed to evaporate for 2–4 days until full dryness. In all cases, the majority of material was still amorphous, and only few single crystals were found to be suitable for X-ray analysis. This way, single crystals of $(NH_4)_2M(PO_3F)_2(H_2O)_2$ (M = Mg, Co, Mn), $(NH_4)_2Ni(PO_3F)_2(H_2O)_6$, $NH_4Cr(PO_3F)_2(H_2O)_6$ and $NH_4Cu_2(H_3O_2)(PO_3F)_2$ could be obtained from the respective metal salt solution. Single crystals of $Cr_2(PO_3F)_3(H_2O)_{18.8}$ were likewise harvested from the batch containing the ammonium-chromium monofluorophosphate solution. From the original ammonium zinc monofluorophosphate solution, three different types of single crystals were isolated, *viz.* $ZnPO_3F(H_2O)_{2.5}$, $(NH_4)_2Zn(PO_3F)_2(H_2O)_{0.2}$ and $(NH_4)_2Zn_3(PO_3F)_4(H_2O)$.

Single crystals of $CdPO_3F(H_2O)_2$ and $Pb_2(PO_3F)Cl_2(H_2O)$ were obtained from metathesis reactions. For this purpose, 200 mg Ag_2PO_3F (prepared according to [4]) were dissolved in 10 mL of water; equimolar amounts of $CdCl_2$ and $PbCl_2$, respectively, were added to the solution, resulting in an immediate precipitation of AgCl. The suspension was stirred for two hours, AgCl filtered off, and the filtrate allowed to evaporate until complete dryness. $CdPO_3F(H_2O)_2$ was obtained as a single phase material, whereas only few single crystals of $Pb_2(PO_3F)Cl_2(H_2O)$ could be isolated. In the latter batch, polycrystalline $2PbCO_3 \cdot Pb(OH)_2$ was also determined by XRPD next to a dark-brown to metallic film deposited at the surface of the glass. The formation of the film points to silver that apparently was also present in the filtrate and was reduced to its metallic form during evaporation.

2.2. Single Crystal Diffraction and Structure Analysis

Single crystals were optically preselected under a polarising microscope, embedded in perfluorinated polyether for protection from air and humidity and mounted on MiTeGen MicroLoops^{TM} for the diffraction studies. Experimental details of the data collections and refinements are collated in Table 1.

All crystal structures were initially solved with SHELXS [12] and refined with SHELXL [13]. For the renewed refinement of $ZnPO_3F(H_2O)_{2.5}$ and $(NH_4)_2Ni(PO_3F)_2(H_2O)_6$, the original atom labelling and atomic coordinates (as starting parameters) were resumed from the original structure reports [14,15]. For $NH_4Cu_2(H_3O_2)(PO_3F)_2$, atom labelling and coordinates were adopted from isotypic $KCu_2(H_3O_2)_3(SO_4)_2$ [16]. In cases where H atom positions were clearly discernible from difference Fourier maps, the corresponding sites were refined with soft restraints on N–H or O–H bond lengths. In cases where H atom positions could not be unambiguously located, H atoms were not considered in the final model, but are part of the chemical formula, X-ray density, etc. These cases apply to $Pb_2(PO_3F)Cl_2(H_2O)$, $Cr_2(PO_3F)_3(H_2O)_{18.8}$ and $(NH_4)_2Zn(PO_3F)_2(H_2O)_{0.2}$. In the crystal structure model of the chromium compound severe disorder of the free water molecules (i.e., the non-coordinating or structural water molecules) is observed, both in terms of occupational and positional disorder; the same applies for the partly hydrated zinc compound. Site occupation factors (s.o.f.) for these O sites were refined freely without restraints or constrains. Disorder was also observed for $NH_4Cr(PO_3F)_2(H_2O)_6$ and $NH_4Cu_2(H_3O_2)(PO_3F)_2$ where the N atom of the ammonium cation is situated on a position with site symmetry $\bar{3}m$ and $2/m$, respectively, which results in a symmetry-restricted disorder of the corresponding ammonium H atoms. Finally, in the crystal structure of $(NH_4)_2Zn_3(PO_3F)_4(H_2O)$, the N site of the ammonium cation and the O site of the water molecule share the same fully occupied site with a 2/3 occupation by N and a 1/3 occupation by O.

Further details of the crystal structure investigations may be obtained from The Cambridge Crystallographic Data Centre (CCDC) on quoting the depository numbers listed at the end of Table 1. The data can be obtained free of charge via www.ccdc.cam.ac.uk/structures.

Table 2 lists selected bond lengths and angles for all crystal structures, and Table 3 gives numerical details of hydrogen bonding.

Table 1. Details of data collections and structure refinements.

Compound		$\mathbf{CdPO_3F(H_2O)_2}$	$\mathbf{Cr_2(PO_3F)_3(H_2O)_{18.8}}$	$\mathbf{Pb_2(PO_3F)Cl_2(H_2O)}$	$\mathbf{ZnPO_3F(H_2O)_{2.5}}$	$\mathbf{(NH_4)_2Co(PO_3F)_2(H_2O)_2}$	$\mathbf{(NH_4)_2Mg(PO_3F)_2(H_2O)_2}$
Formula weight		246.40	736.88	601.27	208.38	326.99	292.37
Temperature/°C		23	−173	23	−173	23	23
Radiation; λ/Å		Mo K$\bar{\alpha}$; 0.71073	Mo K$\bar{\alpha}$; 0.71073	Mo K$\bar{\alpha}$; 0.71073	Mo K$\bar{\alpha}$; 0.71073	Mo K$\bar{\alpha}$; 0.71073	Mo K$\bar{\alpha}$; 0.71073
Diffractometer		SMART CCD	APEX-II CCD	SMART CCD	APEX-II CCD	CAD-4	SMART CCD
Crystal dimensions / mm		0.14 × 0.10 × 0.04	0.10 × 0.10 × 0.01	0.35 × 0.05 × 0.04	0.12 × 0.02 × 0.02	0.05 × 0.05 × 0.01	0.04 × 0.04 × 0.01
Crystal colour; shape		colourless; fragment	green; plate	colourless; needle	colourless; rod	violet; plate	colourless; plate
Space group, no.		$P\bar{1}$, 2	$P\bar{1}$, 2	$Pnma$, 62	$P\bar{1}$, 2	$C2/m$, 12	$C2/m$, 12
Formula units Z		2	4	4	4	2	2
a/Å		5.27680(10)	11.5937(16)	20.4864(14)	7.6020(2)	13.386(3)	13.374(2)
b/Å		6.66970(10)	15.292(2)	5.3967(4)	7.6490(2)	5.3476(9)	5.3541(8)
c/Å		7.7037(2)	15.360(2)	6.9722(5)	9.4671(3)	7.390(2)	7.3852(11)
α/°		65.5060(10)	83.804(6)	90	88.633(2)	90	90
β/°		85.9190(10)	84.203(6)	90	88.888(2)	114.02(2)	113.758(3)
γ/°		75.3940(10)	82.579(6)	90	87.182(2)	90	90
V/Å^3		238.584(9)	2674.1(6)	770.84(10)	549.58(3)	483.2(2)	484.01(13)
μ/mm^{-1}		4.867	1.118	44.496	4.733	2.169	0.576
X-ray density/g·cm^{-3}		3.430	1.830	5.181	2.518	2.247	2.006
Absorption correction		multi-scan; *SADABS*	multi-scan; *SADABS*	multi-scan; *SADABS*	multi-scan; *SADABS*	numerical; *HABITUS*	multi-scan; *SADABS*
Trans. coef. $T_{\min}$; $T_{\max}$		0.549; 0.829	0.778; 0.972	0.023; 0.269	0.545; 0.749	0.884; 0.934	0.887; 0.922
Range $\theta_{\min}$–$\theta_{\max}$		2.91–35.51	1.34–26.00	3.09–30.49	2.15–43.26	3.02–29.96	3.01–28.29
Range	h	−8–7	−14–14	−25–29	−14–14	−18–18	−17–17
	k	−10–10	−18–18	−7–7	−14–14	−7–7	−7–7
	l	−12–12	−18–18	−9–9	−18–18	−10–10	−9–9
Measured reflections		20950	80926	8539	77904	2799	3204
Independent reflections		2055	10504	1291	8190	772	660
Obs.reflections [$I > 2\sigma(I)$]		1927	6720	1176	7431	540	517
R_i		0.0235	0.0731	0.0390	0.0329	0.0668	0.0525
Number of parameters		87	681	59	198	55	55
Ext. coef. (SHELXL)		0.0173(9)	-	0.00298(15)	0.0042(4)	-	-
Diff. elec. dens. max; min [e$^-$·Å^{-3}] (dist./Å, atom)		0.51 (0.70, Cd1); −0.56 (0.65, Cd1)	1.24 (0.94, O8W); −0.97 (0.43, O14W)	2.33 (0.80, Pb1); −1.51 (0.26, Pb2)	1.34 (1.52, O8); −0.48 (0.48, O4)	0.44 (0.49, O1); −0.34 (0.51, H2)	0.57 (0.71, O2); −0.34 (1.23, H2)
$R[F^2 > 2\sigma(F^2)]$		0.0136	0.0605	0.0237	0.0220	0.0280	0.0462
$wR2(F^2$ all)		0.0297	0.2010	0.0554	0.0523	0.0662	0.1153
Goof		1.081	1.036	1.062	1.225	0.989	1.031
CSD number		2,048,140	2,048,141	2,048,144	2,048,145	2,048,134	2,048,135

Table 1. *Cont.*

Compound		**$(NH_4)_2Mn(PO_3F)_2(H_2O)_2$**	**$(NH_4)_2Ni(PO_3F)_2(H_2O)_6$**	**$NH_4Cr(PO_3F)_2(H_2O)_6$**	**$NH_4Cu_2(H_3O_2)(PO_3F)_2$**	**$(NH_4)_2Zn(PO_3F)_2(H_2O)_{0.2}$**	**$(NH_4)_2Zn_3(PO_3F)_4(H_2O)$**
Formula weight		323.00	398.83	374.08	376.09	301.10	642.09
Temperature/°C		−173	−173	−173	−173	23	−173
Radiation; λ/Å		Mo K$\bar{a}$; 0.71073	Mo K$\bar{a}$; 0.71073	Mo K$\bar{a}$; 0.71073	Mo K$\bar{a}$; 0.71073	Mo K$\bar{a}$; 0.71073	Mo K$\bar{a}$; 0.71073
Diffractometer		APEX-II CCD	APEX-II CCD	APEX-II CCD	APEX-II CCD	APEX-II CCD	APEX-II CCD
Crystal dimensions/mm		0.08 × 0.06 × 0.01	0.44 × 0.32 × 0.15	0.15 × 0.15 × 0.08	0.20 × 0.10 × 0.08	0.10 × 0.10 × 0.01	0.08 × 0.08 × 0.08
Crystal colour; shape		light-pink; plate	blue; fragment	green; plate	light-blue; parallelepiped	colourless; plate	colourless; octahedron
Space group, no.		$P2_1/n$, 14	$P2_1/c$, 14	$R\bar{3}m$, 166	$C2/m$, 12	$C2/c$, 15	$I\bar{4}3d$, 220
Formula units Z		2	2	3	2	12	4
a/Å		12.558(3)	6.2700(3)	6.5491(2)	9.1012(8)	18.9363(17)	11.3693(4)
b/Å		5.4559(19)	12.2845(6)	6.5491(2)	6.4121(5)	7.6955(7)	11.3693(4)
c/Å		7.4215(18)	9.1894(4)	25.4381(14)	7.8506(7)	20.5276(18)	11.3693(4)
α/°		90	90	90	90	90	90
β/°		99.918(5)	106.033(2)	90	116.277(3)	108.641(2)	90
γ/°		90	90	120	90	90	90
V/Å^3		500.9(2)	680.27(6)	944.88(8)	410.80(6)	2834.4(4)	1469.61(16)
μ/mm^{-1}		1.697	1.745	1.245	5.631	2.976	5.415
X-ray density/g·cm^{-3}		2.142	1.947	1.972	3.040	2.117	2.902
Absorption correction		multi-scan; *SADABS*	multi-scan; *SADABS*	multi-scan; *SADABS*	multi-scan; *SADABS*	multi-scan; *SADABS*	multi-scan; *SADABS*
Trans. coef. $T_{\min}$; $T_{\max}$		0.636; 0.747	0.662; 0.749	0.661; 0.747	0.631; 0.748	0.889; 0.995	0.656; 0.746
Range $\theta_{\min}$–$\theta_{\max}$		2.98–32.99	2.34–45.97	2.40–34.71	2.89–39.98	2.88–31.00	4.39–30.00
Range	h	−18–19	−12–12	−10–10	−16–16	−27–19	−15–12
	k	−8–8	−24–24	−9–10	−11–11	−11–11	−15–15
	l	−11–11	−18–18	−40–40	−14–13	−23–29	−16–16
Measured reflections		10,452	105,648	6844	7619	11,828	6077
Independent reflections		1886	5910	557	1356	4382	362
Obs.reflections [$I > 2\sigma(I)$]		1059	5659	461	1183	3079	328
R_i		0.0881	0.0227	0.0526	0.0336	0.0392	0.0516
Number of parameters		94	129	30	57	234	33
Ext. coef. (SHELXL)		-	0.0022(9)	-	-	-	-
Flack parameter		-	-	-	-	-	0.026(15)
Diff. elec. dens. max; min		0.56 (0.63, O1)	0.53 (0.56, Ni1);	0.51 (0.77, Cr1);	1.07 (1.52, H1W);	0.78 (0.75, O1);	0.34 (0.78, O1);
[e$^-$·Å^{-3}] (dist./Å, atom)		−0.63 (0.72, P1)	−0.79 (0.55, Ni1)	−0.51 (0.0, Cr1)	−0.83 (0.60, Cu1)	−0.45 (1.36, Zn2)	−0.33 (0.41, Zn1A)
$R[F^2 > 2\sigma(F^2)]$		0.0404	0.0142	0.0232	0.0239	0.0467	0.0265
$wR2(F^2$ all)		0.1009	0.0400	0.0621	0.0575	0.1133	0.0533
Goof		1.012	1.160	1.140	1.109	1.009	1.114
CSD number		2,048,136	2,048,137	2,048,142	2,048,143	2,048,138	2,048,139

Table 2. Selected interatomic distances/Å and angles/°.

$CdPO_3F(H_2O)_2$			
Cd1	OW1	2.2474(10)	
Cd1	O2	2.2505(9)	
Cd1	O1	2.2545(9)	
Cd1	O3	2.2867(9)	
Cd1	O3	2.3310(9)	
Cd1	OW2	2.3865(10)	
P1	O1	1.5058(9)	
P1	O2	1.5073(9)	
P1	O3	1.5155(9)	
P1	F1	1.5747(8)	
O−P1−O		113.89(5)–114.93(5)	
O−P1−F1		103.37(5)–104.33(5)	

$ZnPO_3F(H_2O)_{2.5}$			
Zn1	O10	1.9480(7)	
Zn1	O8	1.9614(8)	
Zn1	O7	1.9647(7)	
Zn1	O5	1.9915(7)	
Zn1	P2	2.9235(3)	
Zn2	O9	2.0199(8)	
Zn2	O9	2.0199(8)	2x
Zn2	O6	2.0941(8)	2x
Zn2	O4	2.1306(8)	2x
Zn3	O3	1.9979(8)	2x
Zn3	O11	2.1130(9)	2x
Zn3	O1	2.1308(8)	2x
P1	O3	1.4866(8)	
P1	O8	1.5123(8)	
P1	O7	1.5342(7)	
P1	F2	1.5604(7)	
P2	O9	1.4906(8)	
P2	O10	1.5167(8)	
P2	O5	1.5302(7)	
P2	F1	1.5595(7)	
O−P−O		109.98(5)–115.78(5)	
O−P−F		103.61(4)–108.61(4)	

$NH_4Cr(PO_3F)_2(H_2O)_6$			
Cr1	O2W	1.9622(10)	6x
P1	O1	1.5106(10)	3x
P1	F1	1.5676(17)	
O1-P-O1		113.44(4)	
O1-P-F1		105.13(4)	

$(NH_4)_2Mn(PO_3F)_2(H_2O)_2$			
Mn1	O3	2.151(2)	2x
Mn1	O1	2.1650(19)	2x
Mn1	O1W	2.240(2)	2x
P1	O1	1.512(2)	
P1	O2	1.5140(19)	
P1	O3	1.517(2)	
P1	F1	1.5944(19)	
O-P-O		112.73(12)–114.98(12)	
O-P-F1		103.15(10)–105.12(10)	

$NH_4Cu_2(H_3O_2)(PO_3F)_2$			
Cu1	O2	1.9493(10)	2x
Cu1	O1H	2.0217(8)	2x
Cu1	O1	2.3642(10)	2x

$Cr_2(PO_3F)_3(H_2O)_{18.8}$			
Cr1	O1	1.956(3)	2x
Cr1	O2	1.960(3)	2x
Cr1	O3	1.973(3)	2x
Cr2	O4	1.949(3)	2x
Cr2	O5	1.959(3)	2x
Cr2	O6	1.971(3)	2x
Cr3	O7	1.939(3)	
Cr3	O8	1.950(4)	
Cr3	O9	1.952(3)	
Cr3	O10	1.969(4)	
Cr3	O11	1.975(4)	
Cr3	O12	1.984(3)	
Cr4	O13	1.947(3)	
Cr4	O14	1.950(4)	
Cr4	O15	1.955(3)	
Cr4	O16	1.972(4)	
Cr4	O17	1.977(3)	
Cr4	O18	1.983(3)	
Cr5	O19	1.942(4)	
Cr5	O20	1.959(4)	
Cr5	O21	1.960(4)	
Cr5	O22	1.967(4)	
Cr5	O24	1.974(4)	
Cr5	O23	1.976(4)	
P1	O11P	1.505(3)	
P1	O12P	1.507(3)	
P1	O13P	1.518(3)	
P1	F1	1.568(3)	
P2	O21P	1.501(4)	
P2	O22P	1.503(4)	
P2	O23P	1.521(3)	
P2	F2	1.564(3)	
P3	O31P	1.498(4)	
P3	O32P	1.511(3)	
P3	O33P	1.521(3)	
P4	F3	1.563(3)	
P4	O41P	1.497(4)	
P4	O42P	1.503(4)	
P4	O43P	1.523(3)	
P5	F4	1.564(3)	
P5	O51P	1.494(4)	
P5	O52P	1.507(4)	
P5	O53P	1.518(3)	
P6	F5	1.564(4)	
P6	O61P	1.480(4)	
P6	O62P	1.483(4)	
P6	O63P	1.519(3)	
P6	F6B	1.585(7)	
P6	F6A	1.591(9)	
O−P−O		113.1(2)–114.6(2)	
O−P−F		90.4(4)–118.9(4)	

$(NH_4)_2Zn(PO_3F)_2(H_2O)_{0.2}$			
Zn1	O9	1.911(3)	
Zn1	O5	1.920(3)	
Zn1	O3	1.929(2)	
Zn1	O2	1.940(2)	
Zn2	O8B	1.835(11)	
Zn2	O8B	1.835(11)	
Zn2	O4A	1.872(5)	
Zn2	O4A	1.872(5)	
Zn2	O8A	1.958(6)	
Zn2	O8A	1.958(6)	
Zn2	O4B	1.988(12)	

$Pb_2(PO_3F)Cl_2(H_2O)$			
Pb1	O1	2.570(3)	2x
Pb1	O1W	2.703(7)	
Pb1	Cl1	2.875(2)	
Pb1	Cl2	2.9423(10)	2x
Pb1	Cl2	3.048(2)	
Pb2	O2	2.301(5)	
Pb2	O1	2.503(3)	2x
Pb2	Cl1	3.1402(10)	2x
Pb2	O2	3.142(3)	2x
Pb2	O1	3.167(3)	2x
P1	O2	1.493(6)	
P1	O1	1.517(4)	2x
P1	F1	1.564(5)	
O−P1−O		111.92(17)–113.9(2)	
O−P1−F1		105.12(19)–108.2(3)	

$(NH_4)_2Co(PO_3F)_2(H_2O)_2$			
Co1	O2	2.0714(16)	4x
Co1	O1W	2.161(3)	2x
P1	O1	1.505(3)	
P1	O2	1.5056(17)	2x
P1	F1	1.579(2)	
O−P1−O		112.54(15)–115.25(8)	
O−P1−F1		103.27(9)–105.39(14)	

$(NH_4)_2Mg(PO_3F)_2(H_2O)_2$			
Mg1	O2	2.0561(18)	4x
Mg1	O1W	2.124(3)	2x
P1	O1	1.501(3)	
P1	O2	1.5045(19)	
P1	F1	1.586(2)	
O−P1−O		113.31(16)–114.74(9)	
O−P1−F1		103.47(9)–105.35(6)	

$(NH_4)_2Ni(PO_3F)_2(H_2O)_6$			
Ni1	O4	2.0295(3)	
Ni1	O6	2.0624(3)	
Ni1	O5	2.0747(3)	
P1	O1	1.5082(3)	
P1	O2	1.5109(3)	
P1	O3	1.5113(3)	
P1	F1	1.6054(3)	
O−P1−O		113.599(17)–115.710(17)	
O−P1−F1		103.168(16)–104.160(18)	

$(NH_4)_2Zn_3(PO_3F)_4(H_2O)$			
Zn1A	O1	1.934(3)	4x
Zn1B	O1	1.766(11)	
Zn1B	O1	1.830(11)	
Zn1B	O1	2.199(10)	
Zn1B	O1W	2.204(14)	
P1	O1	1.497(3)	3x
P1	F1	1.554(5)	
O−P1−O		113.24(13)	
O−P1−F1		105.37(16)	

Table 2. *Cont.*

$CdPO_3F(H_2O)_2$				**$Cr_2(PO_3F)_3(H_2O)_{18.8}$**			**$Pb_2(PO_3F)Cl_2(H_2O)$**
P1	O1	1.5052(14)		Zn2	O4B	1.988(12)	
P1	O2	1.5138(10)	2x	P1	O1	1.484(3)	
P1	F1	1.5934(12)		P1	O2	1.512(2)	
				P1	O3	1.512(2)	
O−P1−O		114.36(8)–114.85(5)		P1	F1	1.575(2)	
O−P1−F1		103.15(5)–104.34(7)		P2	O4B	1.469(12)	
				P2	O5	1.488(3)	
				P2	O6	1.489(3)	
				P2	O4A	1.532(7)	
				P2	F2	1.556(3)	
				P3	O7	1.472(3)	
				P3	O8A	1.485(6)	
				P3	O9	1.498(3)	
				P3	F3	1.556(3)	
				P3	O8B	1.597(13)	
				O−P−O		101.6(4)–127.3(10)	
				O−P−F		86.8(9)–116.2(6)	

Table 3. Details of hydrogen bonding/Å, °.

D	H	A	D–H	H···A	D···A	D–H···A	D	H	A	D–H	H···A	D···A	D–H···A
$CdPO_3F(H_2O)_2$							**$ZnPO_3F(H_2O)_{2.5}$**						
OW1	H1	OW2	0.83(2)	1.99(2)	2.7983(15)	164(2)	O1	H1	O10	0.819(9)	1.960(9)	2.7778(11)	177(2)
OW1	H2	O2	0.81(2)	2.34(3)	2.9231(14)	129(2)	O1	H2	O5	0.819(10)	2.004(10)	2.8212(11)	175(3)
OW1	H2	O1	0.81(2)	2.36(3)	2.9635(14)	133(2)	O2	H3	O1	0.818(10)	2.25(2)	2.9854(14)	149(3)
OW2	H3	O2	0.90(2)	2.00(2)	2.8740(15)	162(2)	O2	H4	O4	0.814(10)	2.496(15)	3.2526(14)	155(3)
OW2	H3	F1	0.90(2)	2.57(3)	3.1411(14)	121(2)	O2	H4	O6	0.814(10)	2.52(2)	3.1410(13)	134(2)
OW2	H4	O1	0.84(2)	2.18(2)	3.0032(15)	167(2)	O4	H5	O2	0.823(9)	1.992(11)	2.8053(13)	170(3)
OW2	H4	F1	0.84(2)	2.60(2)	3.0887(13)	118(2)	O4	H6	O5	0.828(9)	2.047(10)	2.8707(11)	173(2)
							O6	H7	O8	0.816(9)	1.900(10)	2.7136(11)	175(2)
$(NH_4)_2Co(PO_3F)_2(H_2O)_2$							O6	H8	O7	0.818(9)	2.018(10)	2.8336(11)	174(2)
N1H	H1	O1	0.92(4)	1.88(4)	2.800(4)	180(5)	O11	H9	O7	0.819(10)	2.059(11)	2.8641(11)	168(3)
N1H	H2	O2	0.86(4)	2.22(3)	2.924(3)	139.9(8)	O11	H10	O2	0.822(10)	2.059(10)	2.8742(13)	171(3)
N1H	H3	O2	0.85(3)	2.32(3)	3.031(4)	142(3)							
O1W	H4	O1	0.81(3)	2.14(3)	2.8702(14)	149(3)	**$(NH_4)_2Ni(PO_3F)_2(H_2O)_6$**						
							N1	H1N	O3	0.849(12)	2.159(12)	2.9613(5)	157.6(11)
$(NH_4)_2Mg(PO_3F)_2(H_2O)_2$							N1	H2N	O3	0.917(11)	1.921(11)	2.8283(4)	169.8(10)
N1H	H1	O1	0.90(4)	1.90(4)	2.801(5)	175(5)	N1	H3N	O1	0.896(12)	1.921(12)	2.8134(5)	173.7(10)
N1H	H2	O2	0.88(4)	2.21(3)	2.933(4)	139.7(9)	N1	H4N	O2	0.849(11)	2.115(11)	2.9053(5)	154.7(10)
N1H	H3	O2	0.82(3)	2.34(4)	3.040(4)	143(4)	O4	H5W	O3	0.834(10)	1.866(10)	2.6969(4)	174.0(11)
O1W	H4	O1	0.76(3)	2.15(3)	2.8732(16)	160(4)	O4	H6W	O1	0.826(11)	1.938(11)	2.7489(4)	167.0(10)
							O5	H7W	O2	0.799(11)	1.883(11)	2.6792(4)	173.7(11)
$(NH_4)_2Mn(PO_3F)_2(H_2O)_2$							O5	H8W	F1	0.804(11)	2.010(11)	2.8146(4)	178.6(12)
O1W	H1W	O2	0.850(10)	1.930(14)	2.748(3)	161(3)	O6	H9W	O1	0.805(12)	1.956(12)	2.7589(4)	175.3(11)
O1W	H2W	O2	0.849(10)	2.44(3)	3.103(3)	136(4)	O6	H10W	O2	0.789(11)	2.001(11)	2.7874(4)	174.1(11)
N1H	H1N	O1	0.899(10)	2.131(19)	2.945(3)	150(3)							
N1H	H2N	F1	0.897(10)	2.50(3)	3.041(3)	119(3)	**$NH_4Cu_2(H_3O_2)(PO_3F)_2$**						
N1H	H2N	O1W	0.897(10)	2.59(3)	3.209(3)	127(3)	O1H	H1O	F1	0.837(10)	2.344(10)	3.1797(18)	177(4)
N1H	H3N	O2	0.902(10)	1.909(11)	2.810(3)	176(3)	O1H	H2O	O1H	0.999(10)	1.50(4)	2.489(3)	169(20)
N1H	H4N	O3	0.900(10)	1.912(12)	2.803(3)	170(3)	N1	H1N	O2	0.8999(10)	2.021(18)	2.8448(10)	152(3)
							N1	H2N	F1	0.9000(10)	2.24(6)	2.9730(13)	139(8)
							N1	H2N	O1	0.9000(10)	2.03(4)	2.8554(14)	152(8)
$NH_4Cr(PO_3F)_2(H_2O)_6$													
O2W	H1	O1	0.864(16)	1.753(16)	2.6124(9)	173.1(16)	**$(NH_4)_2Zn_3(PO_3F)_4(H_2O)$**						
N1H	H2	O1	0.95(4)	2.00(4)	2.9493(10)	176(3)	N1H/O1W	H1	F1	1.02(8)	2.31(8)	3.1703(11)	141(6)
							N1H/O1W	H1	O1	1.02(8)	2.40(8)	3.007(3)	117(6)

Table 3. *Cont.*

D	H	A	D–H	H···A	D···A	D–H···A	D	H	A	D–H	H···A	D···A	D–H···A
$(NH_4)_2Zn(PO_3F)_2(H_2O)_{0.2}$							N1H/O1W	H1	O1	1.02(8)	2.38(9)	3.190(4)	136(7)
N1	H1	O7	0.897(10)	1.874(16)	2.756(5)	167(5)							
N1	H2	O1	0.891(10)	2.17(3)	2.955(5)	147(5)							
N1	H3	O3	0.898(10)	2.130(18)	3.000(4)	163(5)							
N1	H4	O6	0.894(10)	1.992(14)	2.878(5)	171(5)							
N2	H5	O6	0.897(10)	2.015(18)	2.890(4)	164(5)							
N2	H6	O2	0.896(10)	2.16(2)	3.000(4)	156(4)							
N2	H6	O9	0.896(10)	2.74(4)	3.321(5)	123(4)							
N2	H7	O6	0.899(10)	1.925(13)	2.817(5)	172(5)							
N2	H8	O8A	0.897(10)	1.96(2)	2.811(8)	158(5)							
N2	H8	O8B	0.897(10)	2.49(4)	3.28(3)	148(5)							
N3	H11	O1	0.894(10)	2.08(3)	2.869(5)	146(4)							
N3	H9	O7	0.899(10)	1.89(2)	2.743(5)	158(5)							
N3	H10	O4A	0.897(10)	2.165(16)	3.055(9)	171(4)							
N3	H10	O8B	0.897(10)	2.55(5)	3.03(2)	114(4)							
N3	H12	O1	0.892(10)	1.949(13)	2.837(5)	173(5)							

2.3. Vibrational Spectroscopy

The infrared (IR) spectrum of a powdered $CdPO_3F(H_2O)_2$ sample was recorded as a KBr pellet in the spectral range between 4000 and 400 cm^{-1} employing a Bruker-EQUINOX-55 FTIR-instrument (Billerica, MA, USA). Raman spectra down to 100 cm^{-1}, were measured using the FRA 106 Raman accessory of an IF66 Bruker spectrophotometer (Billerica, MA, USA). Radiation from a Nd:YAG solid-state laser (1064 nm) was used for excitation. The spectral resolution was $\pm$ 4 cm^{-1} in both measurements.

2.4. Thermogravimetry (TG)

A Netzsch TG209 F1 thermobalance (Selb, Germany) was used for measurement using a corundum crucible in flowing nitrogen atmosphere and a heating rate of 20 °C/min.

3. Results

In the current study, only $(NH_4)_2Mg(PO_3F)_2(H_2O)_2$ and $CdPO_3F(H_2O)_2$ were obtained as pure and crystalline phases and in amounts sufficient for the application of other current analytical methods (vibrational spectroscopy, thermogravimetry). All other monofluorophosphates either were obtained in form of multi-phase material or in form of only few single crystals next to amorphous material. This allowed in all cases the determination of the crystal structure but prevented further analytical measurements.

3.1. $CdPO_3F(H_2O)_2$

All atoms in the crystal structure of $CdPO_3F(H_2O)_2$ are located on general sites. The cadmium cation exhibits a distorted octahedral coordination sphere defined by two *cis*-aligned water molecules (OW1, OW2) and four O atoms from four PO_3F^{2-} anions. Two $[CdO_4(OH_2)_2]$ octahedra share an edge to form a dimer $\{Cd_2O_6(OH_2)_4\}$; adjacent dimers are linked by corner-sharing with PO_3F^{2-} groups into layers extending parallel (001). An intralayer hydrogen bond between two water molecules (OW1 and OW2) consolidates this arrangement. Neighbouring layers are held together by medium-strong to weak and partly bifurcated hydrogen bonds between both water molecules and O1 and O2 atoms of the monofluorophosphate anions (Figure 1).

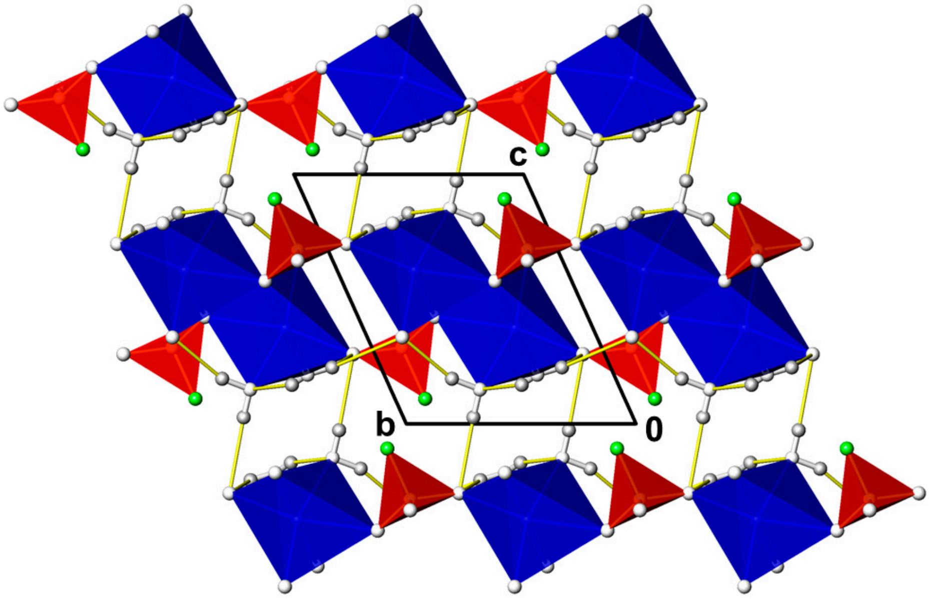

Figure 1. The crystal structure of $CdPO_3F(H_2O)_2$ in a projection along $[\bar{1}00]$. PO_3F tetrahedra are given in red (O atoms as colourless, F atoms as green spheres), $[CdO_6]$ octahedra are given in blue, and H atoms are given as grey spheres. O–H···O hydrogen bonding is indicated by yellow lines.

On the basis of the known structural data, it is possible to perform an analysis of the vibrational-spectroscopic behaviour of the PO_3F^{2-} anion present in the $CdPO_3F(H_2O)_2$ crystal structure, using the simple site-symmetry approximation [17–20]. Since the monofluorophosphate anion is located on a general C_1 position, the symmetry of the "free" PO_3F^{2-} anion (C_{3v}) was correlated with its site symmetry (C_1), as shown in Table 4. From these results, it becomes evident that, under site symmetry conditions, the three double degenerated E modes are split, and all vibrations present IR and Raman activity. The FTIR spectrum of $CdPO_3F(H_2O)_2$ is quite simple (Figure 2a) and can be clearly correlated with the results of this analysis. In the Raman spectrum, a more reduced number of bands was observed which, notwithstanding, was useful to additionally support the performed assignments, which are shown in Table 4 and briefly commented on as follows:

- Regarding the vibrations of the water molecules, the O–H stretchings are seen as a relatively broad and clearly splitted band due to the presence of two crystallographically different water molecules. The positions of these bands are characteristic for the presence of hydrogen bridges of medium strength [20], in agreement with the results of the structure analysis. Interestingly, the corresponding deformational mode, $\delta(H_2O)$, shows also splitting signals.
- The antisymmetric $\nu(PO_3)$ vibration was not observed in the Raman spectrum, whereas in the IR spectrum it is very strong and broad. In accord with the predictions of the site-symmetry analysis two components can be seen. The corresponding symmetric stretching vibration is the strongest Raman band in both compounds and is also relatively strong in the IR spectrum.
- The ν(P–F) vibration can be clearly identified in the spectra, lying at somewhat higher energy than that observed in the solution Raman spectrum (795 cm^{-1}) [20].
- For the deformational modes only $\delta(PO_3)$ could be identified, clearly split in the IR spectra as predicted (cf. Table 4), whereas no signals for the $\delta(FPO_3)$ mode could be found. In the Raman spectrum of a PO_3F^{2-} solution, both vibrations are reported at the same energy (520 cm^{-1}) [20], although in the case of crystalline Hg_2PO_3F, both vibrations were identified at slightly different wavenumbers, with $\nu_5 > \nu_3$ [21].
- The corresponding ν_6-PO_3-rocking mode was only identified in the Raman spectrum, as a very weak band.

Table 4. Site symmetry analysis of the PO_3F^{2-} vibrations in the lattice of $CdPO_3F(H_2O)_2$ and assignment of IR and Raman bands (band positions in cm^{-1}).

	Vibrational Mode	Free Anion (C_{3v})	Site Symmetry (C_1)	IR	Raman
ν_1	ν(P–F)	A_1	A	825 vs	826 m
ν_2	$\nu_s(PO_3)$	A_1	A	1006 vs	1022 vs
ν_3	$\delta(FPO_3)$	A_1	A		
ν_4	$\nu_{as}(PO_3)$	E	2A	1142 vs, 1106 vs	—
ν_5	$\delta(PO_3)$	E	2A	560 sh, 541 s	540 w
ν_6	$\varrho(PO_3)$	E	2A	—	395 w
	ν(OH)			3496 vs, 3393 vs, 3223 sh	—
	$\delta(H_2O)$			1648 sh, 1626 m	—

Activity: A_1, E: IR and Raman; A: IR and Raman. Intensity: vs: very strong; s: strong; m: medium; w: weak; sh: shoulder.

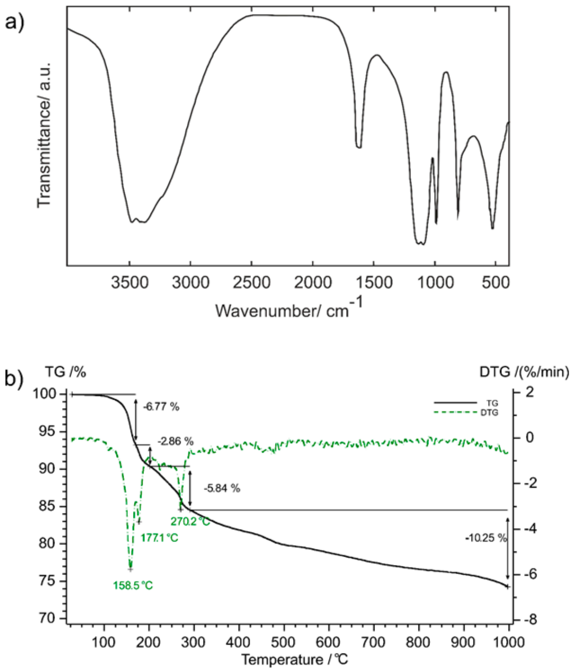

Figure 2. $CdPO_3F(H_2O)_2$. (**a**) IR spectrum; (**b**) TG curve (black) with its fist derivative (DTG curve, green).

The TG curve of $CdPO_3F(H_2O)_2$ and the associated difference curve ist depicted in Figure 2b. The dihydrate starts to decompose with an onset temperature of 144 °C accompanied with a first dehydration step that can be grouped into two separated events. Considering a mass loss of 7.3% per water molecule in the formula unit, the first dehydration event is associated with the loss of about one water molecule (maximum in the difference curve at 159 °C and a mass loss of 6.8%), followed by a second event (maximum in the difference curve at 177 °C) with the release of about one-third of a water molecule (2.9%) relative to the formula unit. The second dehydration step (maximum in the difference curve at 270 °C) is indicated by the release of about two-thirds of a water molecule per formula unit with a further mass loss of 5.8%. The formation of the anhydrous compound is completed at 280 °C (expected overall mass loss 14.6%, observed 15.5%). Above this temperature, the remaining phase(s) gradually decompose(s), and $Cd_2P_2O_7$ [22] was identified by PXRD as the only crystalline reaction product obtained at 1000 °C. For a clear interpretation of this last decomposition step, coupled mass-spectroscopic studies of the gaseous products released during the TG experiment and temperature-dependent PXRD would have been required. In general, monofluorophosphates show a rather complex thermal decomposition behaviour, as exemplified by the cases of $(NH_4)_2Mg(PO_3F)_2(H_2O)_2$ [23] with $Mg_2P_4O_{12}$, of Ag_2PO_3F [4] with $Ag_4P_2O_7$ and Ag_3PO_4, and of $SrPO_3F(H_2O)$ [24] with $Sr_2P_2O_7$ and $Sr_5(PO_4)_3F$, respectively, as the final products.

3.2. $Cr_2(PO_3F)_3(H_2O)_{18.8}$

The crystal structure of $Cr_2(PO_3F)_3(H_2O)_{18.8}$ is rather complex, with five Cr sites (two of which (Cr1, Cr2) are situated on inversion centres on Wyckoff positions 1*a* and 1*h*, respectively), with six PO_3F^{2-} anions (one of which (P6) shows positional disorder of the F6 atom over two set of sites), with 24 O atoms associated with aqua ligands of the Cr(III) atoms, and with 14 crystal water molecules (five of which (O1W–O5W) are positionally and occupationally disordered over multiple sites).

The five chromium(III) atoms are solely ligated by water molecules in an octahedral manner and are isolated in the crystal structure. The corresponding Cr–O_{water} distances are normal and agree with other $[Cr(OH_2)_6]$ octahedra, e.g., like those found in alums [25].

$[Cr(OH_2)_6]$ octahedra associated with Cr3, Cr4, and Cr5 are arranged in (011) layers that are sandwiched by the six monofluorophosphate anions, giving an overall composition of $\{[Cr(OH_2)_6]_3(PO_3F)_6\}^{3-}$. Interestingly, all F atoms of the monofluorophosphate tetrahedra point away from the intermediate cationic layer. The two remaining $[Cr(OH_2)_6]$ octahedra, associated with the two chromium sites Cr1 and Cr2, lie in-between adjacent $\{[Cr(OH_2)_6]_3(PO_3F)_6\}^{3-}$ layers. Together with the partly disordered water molecules O1W-O5W they define an own layer with composition $\{[Cr(OH_2)_6](H_2O)_{13.6}\}^{3+}$. Both types of layers alternate and stack along [011] (Figure 3). Although H atoms could not be located for the water molecules, it is evident that hydrogen bonding is the crucial force for stabilising the stacking arrangement in this crystal structure. Within an anionic $\{[Cr(OH_2)_6]_3(PO_3F)_6\}^{3-}$ layer the aqua ligands most probably are involved in hydrogen bonding to the monofluorophosphate O atoms and also among each other; in the intermediate $\{[Cr(OH_2)_6](H_2O)_{13.6}\}^{3+}$ layer hydrogen bonds might occur between aqua ligands and crystal water molecules. From the same orientation of all monofluorophosphate F atoms towards the $\{[Cr(OH_2)_6](H_2O)_{13.6}\}^{3+}$ layers one might expect also O–H···F hydrogen bonds in this crystal structure. However, a clear localisation of (disordered) H atoms will be possible only by the application of neutron diffraction, provided that crystals large enough for this diffraction technique can be grown.

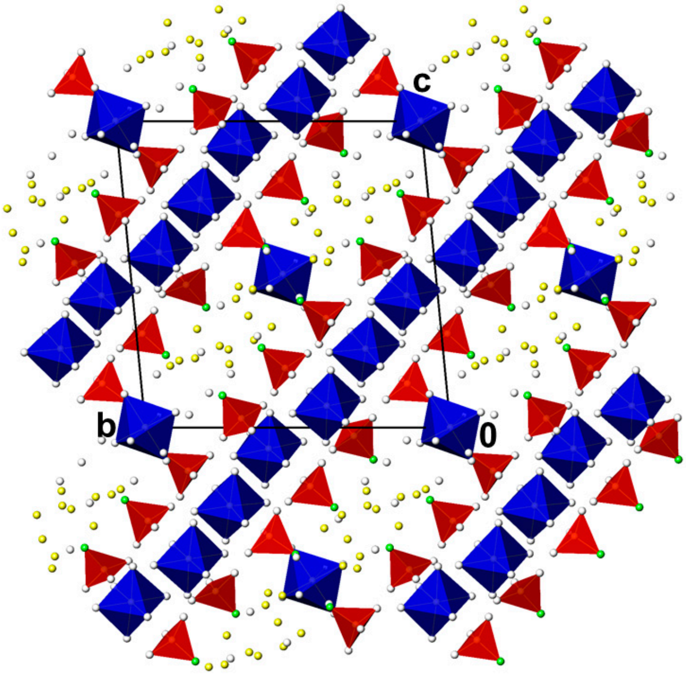

Figure 3. The crystal structure of $Cr_2(PO_3F)_3(H_2O)_{18.8}$ in a projection along $[\bar{1}00]$. Colour code of PO_3F tetrahedra as in Figure 1; $[CrO_6]$ octahedra are given in blue, O atoms of crystal water molecules with full occupation are given as colourless spheres and those of disordered crystal water molecules as yellow spheres. For clarity, disorder of one of the PO_3F groups is not shown.

The formula of this compound can also be written as $[Cr(H_2O)_6]_2(PO_3F)_3{\cdot}6.8H_2O$. Considering full occupancy of the positionally and occupationally disordered five crystal water sites, this would result in a ‚19-hydrate‘, i.e., $[(Cr(H_2O)_6]_2(PO_3F)_3{\cdot}7H_2O$. This amount of water is close to that reported for highly hydrated violet chromium(III) sulfates that are described to contain about 18 water molecules [26]. However, crystal structure determinations of corresponding chromium(III) sulfate hydrates have not been performed up to now.

3.3. *$Pb_2(PO_3F)Cl_2(H_2O)$*

The crystal structure of $Pb_2(PO_3F)Cl_2(H_2O)$ comprises two unique lead(II) atoms, two chloride anions, one monofluorophosphate anion and one water molecule of an aqua ligand. Except one oxygen atom of the latter (O2; H atom(s) could not be determined), all other atoms are situated on a mirror plane (Wyckoff position 4*c*). The two lead(II) atoms exhibit different coordination environments whereby in each case the F atom of the monofluorophosphate anion is not part of the first coordination sphere (shortest Pb–F distances are 3.624(3) Å for Pb1 and 3.912(3) Å for Pb2). Pb1 has a coordination number of 7 (considering distances less than 3.5 Å) and is bonded to two monofluorophosphate O atoms, the O atom of the aqua ligand and four chloride anions. Pb2 has a coordination number of 9, with one very short and two short distances to monofluorophosphate O atoms, two bonds to chloride anions and two pairs of long bonds to monofluorophosphates O atoms. The corresponding $[Pb1O_2(H_2O)Cl_4]$ and $[Pb2O_7Cl_2]$ polyhedra are irregular and share vertices and edges to build up a three-dimensional framework structure (Figure 4). The water molecules protrude into the interstices present in this framework. The monofluorophosphate tetrahedron shares all its O atoms with the framework, whereby the P and F atoms are also oriented towards the interstices of the framework. The next nearest distance between two water molecules in this section of the structure amounts to 3.102(7) Å; three shorter distances to the monofluorophosphate F atom (2.848(8) Å and twice 3.007(4) Å) are also present, making O–H···O and also O–H···F hydrogen bonding interactions possible. Since H atoms could not be determined, detailed hydrogen bonding interactions cannot be provided.

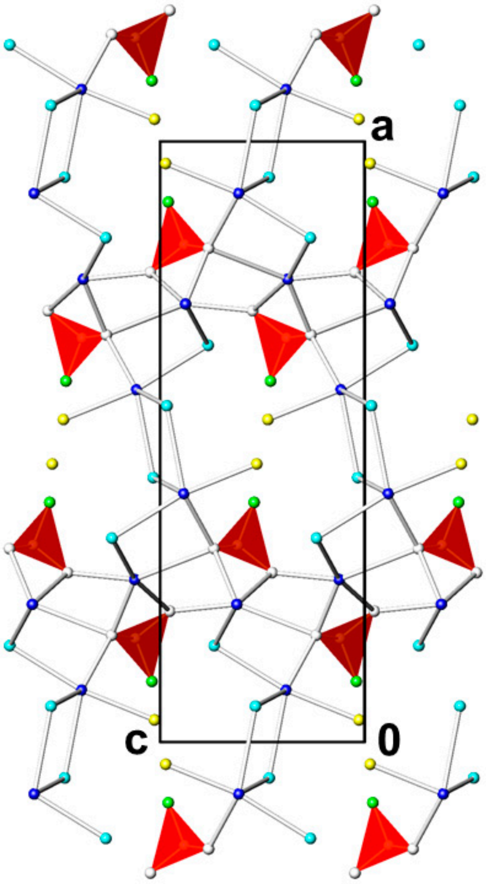

Figure 4. The crystal structure of $Pb_2(PO_3F)Cl_2(H_2O)$ in a projection along $[0\bar{1}0]$. Colour code of PO_3F tetrahedra as in Figure 1; Pb atoms are represented by dark-blue spheres, Cl atoms as turquoise spheres and O atoms of the water molecules as yellow spheres.

3.4. $ZnPO_3F(H_2O)_{2.5}$

The crystal structure of $ZnPO_3F(H_2O)_{2.5}$ has been determined previously from a single crystal X-ray data set at room temperature, using a CAD-4 four-circle diffractometer equipped with a point detector. Since only parts of the water hydrogen atoms could be located at that time [14], the crystal structure model remained incomplete, in particular in terms of hydrogen-bonding interactions. The current re-refinement unambiguously revealed all hydrogen atoms, making a complete assignment of hydrogen-bonding interactions possible.

Two of the three unique zinc cations (Zn2, Wyckoff position 1*h* and Zn3, Wyckoff position 1*a*) are located on inversion centres; all other atoms are in general sites. Zn1 has a tetrahedral coordination environment and is bonded to the O atoms of four monofluorophosphate tetrahedra. Two such units dimerise into an inversion-symmetric $\{Zn1_2(PO_3F)_6\}$ unit. Both Zn2 and Zn3 atoms have an octahedral coordination environment, being bound to two monofluorophosphate O and four water O atoms. The corresponding $[ZnO_2(OH_2)_4]$ octahedra share the non-water O atoms with the $\{Zn1_2(PO_3F)_6\}$ units to define a three-dimensional framework structure. O–H···O hydrogen bonding of medium strengths between the coordinating water molecules and the monofluorophosphate O atoms reinforces this arrangement. There is an additional crystal water molecule (O2) present in the structure acting both as a donor and an acceptor group. O2 donates weak hydrogen bonds (partly bifurcated) to two ligand water O and one monofluorophosphate O atoms, and accepts medium-strong hydrogen bonds of two coordinating water molecules (Figure 5).

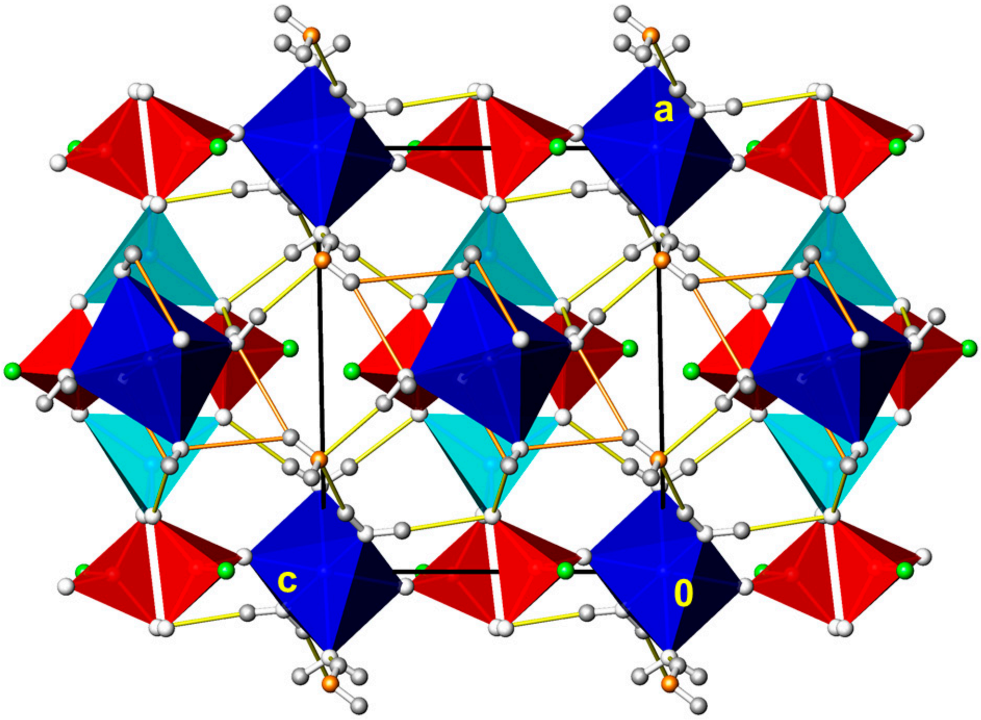

Figure 5. The crystal structure of $ZnPO_3F(H_2O)_{2.5}$ in a projection along [010]. Colour code of PO_3F tetrahedra and H atoms as in Figure 1; $[ZnO_6]$ octahedra are given in dark-blue, $[ZnO_4]$ tetrahedra in turquoise and the O atom of the crystal water molecule as an orange sphere. O–H···O hydrogen bonding with the aqua ligands as donor groups is given as yellow lines, and involving the crystal water molecules as donor groups as orange lines.

3.5. $(NH_4)_2M(PO_3F)_2(H_2O)_2$ (M = Co, Mg)

$(NH_4)_2Co(PO_3F)_2(H_2O)_2$ and $(NH_4)_2Mg(PO_3F)_2(H_2O)_2$ crystallize isotypically with the copper member $(NH_4)_2Cu(PO_3F)_2(H_2O)_2$ in space group $C2/m$ [27]. Instead of the C-centred unit cell for this structure type, PDF entry #00-045-0355 for $(NH_4)_2Co(PO_3F)_2(H_2O)_2$ reports a primitive unit cell (without further assignment of possible space groups) with lattice parameters of a = 12.3817(1), b = 5.3449(5), c = 7.3894(6) Å, β = 98.930(8)°, V = 483.10 Å^3. Comparison with the current single crystal X-ray study (Table 1) revealed virtually the same lengths of the b and c axes and the same unit cell volume. Preparation, chemical analysis as well as infra-red spectroscopic measurements and thermal behaviour of $(NH_4)_2Mg(PO_3F)_2(H_2O)_2$ were already reported some time ago, without determination of the crystal structure. The originally given lattice parameters (a = 15.476(4), b = 5.372(1), c = 13.416(3) Å, β = 118.76(1)°; determined from polycrystalline material using a Guinier camera) and two possible space groups (Cc or $C2/c$) [23] do not match with the current single crystal data with a halved unit cell volume (978 Å^3 for [23] versus 484 Å^3 in the current singly crystal study) and space group $C2/m$. Nevertheless, the deposited X-ray powder diffraction data (PDF entry #00-039-029) can be indexed with the actual halved cell. Rietveld refinement of $(NH_4)_2Mg(PO_3F)_2(H_2O)_2$ unambiguously showed the correctness of the halved cell in space group $C2/m$ (PDF entry #00-059-0045; no structure data given).

The metal cation in the $(NH_4)_2M(PO_3F)_2(H_2O)_2$ (M = Co, Cu, Mg) structure is situated on Wyckoff position 2c with site symmetry $2/m$ and thus has four equal M–O bonds to the O2 atoms of four PO_3F^{2-} anions and two equal bonds to two *trans*-aligned water molecules (O1W). The monofluorophosphate anion is located about a mirror plane, just like the ammonium cation. Adjacent $[MO_4(OH_2)_2]$ octahedra are linked by corner-sharing with the PO_3F^{2-} anions into $\{Mg(OH_2)(PO_3F)_2)^{2-}\}_n$ strands running along [010]. Adjacent strands are aligned in parallel and are arranged into layers along (001). Within a strand, medium-strong hydrogen bonds between the water molecules and the non-coordinating O1 atom of the PO_3F^{2-} anion are established. The ammonium cations are situated between the strands and are hydrogen-bonded to the O1 and O2 atoms of the anions into a three-dimensional network (Figure 6).

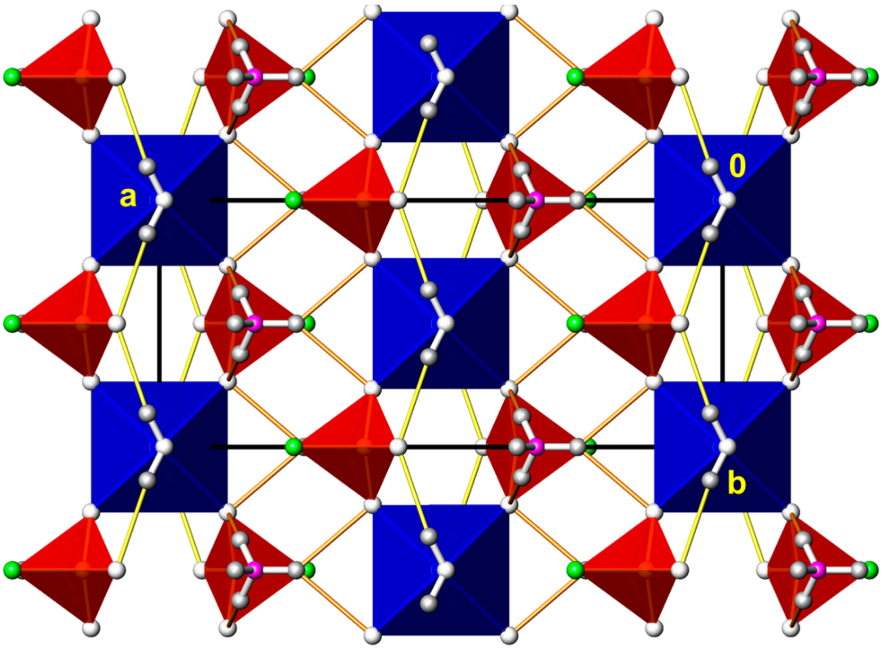

Figure 6. The crystal structure of $(NH_4)_2M(PO_3F)_2(H_2O)_2$ (M = Mg, Co; data used from the Mg-compound) in a projection along [001]. Colour code of PO_3F tetrahedra, H atoms and O–H···O hydrogen bonding as in Figure 1; $[MO_6]$ octahedra are given in blue, N atoms of the ammonium groups as magenta spheres. N–H···O hydrogen bonding is indicated by orange lines.

3.6. $(NH_4)_2Mn(PO_3F)_2(H_2O)_2$

Although manganese is part of the first-row transition metals, $(NH_4)_2Mn(PO_3F)_2(H_2O)_2$ does not adopt the $(NH_4)_2Cu(PO_3F)_2(H_2O)_2$ structure type in space group $C2/m$ described above for the transition metals cobalt and copper. The manganese compound shows a group-subgroup relation with the $(NH_4)_2Cu(PO_3F)_2(H_2O)_2$ structure type, crystallizing in space group $P2_1/n$ that is a klassengleiche subgroup of index 2 [28]. Hence, some of the sites and/or groups in the higher-symmetric space group $C2/m$ have a reduced symmetry or split into two positions in the $P2_1/n$ structure. The divalent metal position (Wyckoff position 2*c*) now shows site symmetry $\overline{1}$, and all other atoms are located on general sites (Wyckoff positions 4*e*). The general features of the $(NH_4)_2Mn(PO_3F)_2(H_2O)_2$ crystal structure (Figure 7) are the same as for the $(NH_4)_2Cu(PO_3F)_2(H_2O)_2$ structure type. $\{Mn(OH_2)(PO_3F)_2)^{2-}\}_n$ strands run along [010] with the water molecule hydrogen-bonded to the non-coordinating O atom of the monofluorophosphate anions; adjacent strands are organised into layers parallel (101). The ammonium cations again are hydrogen-bonded to the strands by weak hydrogen bonds. As expected, the Mn–O bond lengths are the longest in all four $(NH_4)_2M(PO_3F)_2(H_2O)_2$ structures because Mn has the largest ionic radius of all divalent transition metal cations. Most probably, the large ionic radius of Mn^{2+} is the driving force for the symmetry reduction from $C2/m$ to $P2_1/n$.

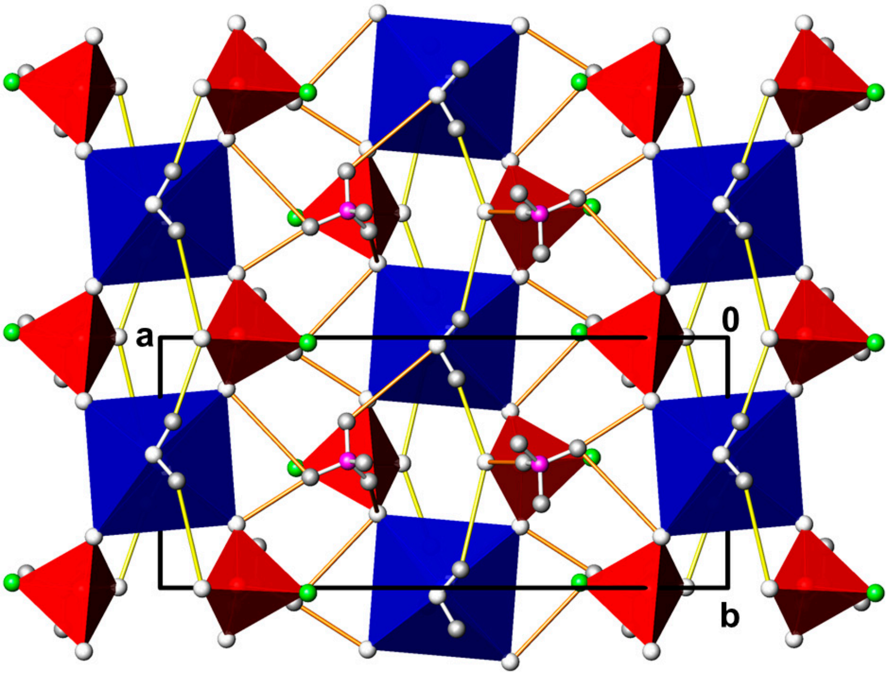

Figure 7. The crystal structure of $(NH_4)_2Mn(PO_3F)_2(H_2O)_2$ in a projection along [001]. Colour code as in Figure 6.

3.7. $(NH_4)_2Ni(PO_3F)_2(H_2O)_6$

In contrast to the ammonium transition metal monofluorophosphate dihydrates $(NH_4)_2M(PO_3F)_2(H_2O)_2$ (M = Mg, Mn, Co, Cu) described in the preceding sections, the nickel compound crystallizes with six water molecules. $(NH_4)_2Ni(PO_3F)_2(H_2O)_6$ is a member of the vast family of Tutton salts with general formula $M^I{}_2M^{II}(XO_4)_2(H_2O)_6$. Typical crystal-chemical features of Tutton salts have been reviewed in various reports, e.g., ([29], and references therein). In short, the unit cell of a Tutton salt comprises two formula units and is made up of one M^{II} site (here Ni) located on a centre of inversion (Wyckoff position 2*a*) and surrounded by six water molecules in the form of a slightly distorted octahedron, one XO_4 tetrahedron (here PO_3F), and one ammonium cation (for cases with other M^I cations distorted M^IO_8 polyhedron are present). Hydrogen bonds of medium strengths between the building units of the type O–H···O and, as a peculiarity in the case of $(NH_4)_2Ni(PO_3F)_2(H_2O)_6$, also of the type O–H···F generate a three-dimensional network structure. The crystal structure of $(NH_4)_2Ni(PO_3F)_2(H_2O)_6$ has previously been determined based on a X-ray diffraction data set recorded at room temperature using a CAD-4 four-circle diffractometer and a point detector. Since the crystal intensities dropped by up to 73% of their initial values during the long-lasting data collection [15], it was decided to re-refine the crystal structure with CCD data at 100 K for an improved model. In principle, the current low-temperature data confirm the previous room-temperature data, however with much higher precision as indicated by standard uncertainties for bond lengths and angles about three to five times smaller. The crystal structure of $(NH_4)_2Ni(PO_3F)_2(H_2O)_6$ is depicted in Figure 8.

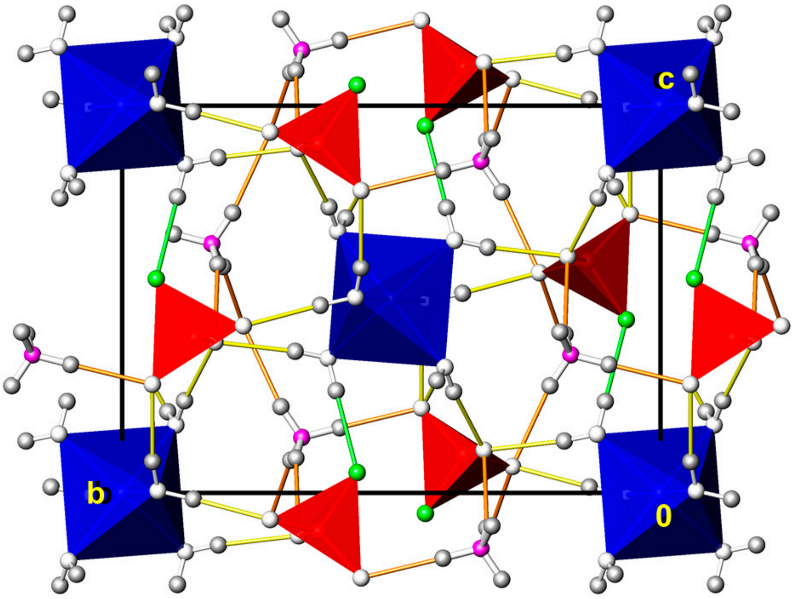

Figure 8. The crystal structure of $(NH_4)_2Ni(PO_3F)_2(H_2O)_6$ in a projection along $[\bar{1}00]$. Colour code as in Figure 6; O–H···F hydrogen bonding is indicated by green lines.

3.8. $NH_4Cr(PO_3F)_2(H_2O)_6$

PDF entry #00-044-0535 reports the same *R*-centred cell for $NH_4Cr(PO_3F)_2(H_2O)_6$ but with space group $R3$ instead of $R\bar{3}m$ determined from the present single crystal X-ray data. In the crystal structure, isolated $[Cr(OH_2)_6]$ octahedra (point group symmetry $\bar{3}m$) are organised in layers parallel (001) and are sandwiched by double layers of PO_3F^{2-} anions (point group symmetry $3m$) along the [001] stacking direction. The disordered ammonium cations (site symmetry $\bar{3}m$) are situated between the PO_3F^{2-} anions in the middle of the monofluorophosphate double layer. Strong hydrogen bonds between the $[Cr(OH_2)_6]$ octahedra and the O atoms of the monofluorophosphate groups link the chromium and monofluorophosphate layers together. Ammonium cations additionally hydrogen-bond to the O atoms within a monofluorophosphate double layer (Figure 9).

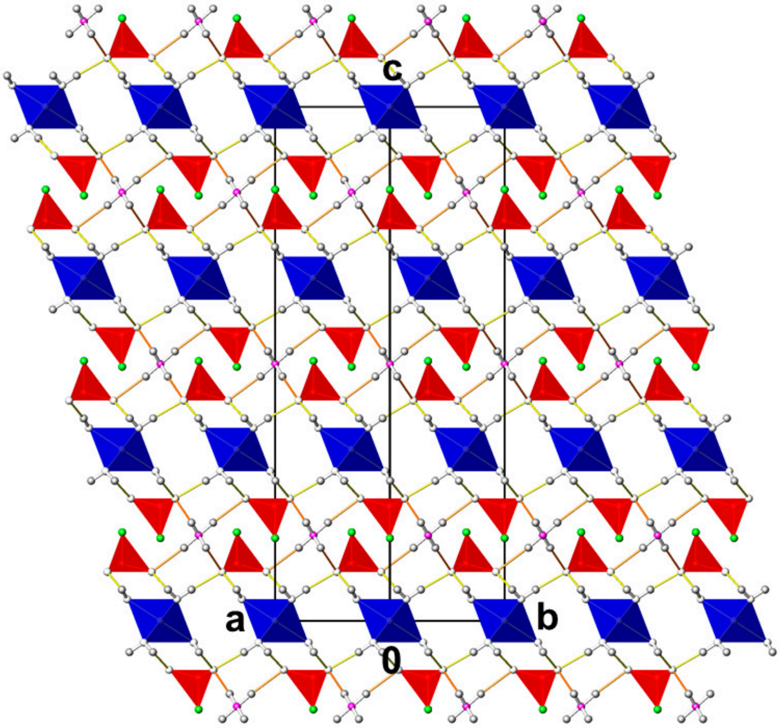

Figure 9. The crystal structure of $NH_4Cr(PO_3F)_2(H_2O)_6$ in a projection along [110]. Colour code as in Figure 6.

3.9. $NH_4Cu_2(H_3O_2)(PO_3F)_2$

The ammonium copper compound crystallizes isotypically with $KCu_2(H_3O_2)(PO_3F)_2$ [30] in the natrochalcite structure type [16]. The copper cation (site symmetry $2/m$; Wyckoff position 4*e*) is surrounded by six O atoms and shows its characteristic tetragonally distorted octahedral coordination owing to the Jahn-Teller effect. Neighbouring $[CuO_6]$ polyhedra share common edges to form chains parallel to [010]. Adjacent chains are bridged by the monofluorophosphate tetrahedra (site symmetry *m*), sharing exclusively the O atoms into (001) layers. The disordered ammonium cation (with the N atom situated on Wyckoff position 2*d* with site symmetry $2/m$) is located between adjacent layers and links them through hydrogen bonding to the monofluorophosphate O atoms. Additional hydrogen bonds, albeit of weak nature, develop between the non-disordered part of the $\{H_3O_2\}^-$ group and the F atom of the monofluorophosphate anion. The crystal structure is shown in Figure 10. It is well known that natrochalcite-type compounds contain such $\{H_3O_2\}^-$ groups where a positionally disordered H atom with half-occupation (here H2O) sits between two OH^- groups. Since the features of the resulting hydrogen bonding system, including a clear location of hydrogen atoms by neutron diffraction, was reported for isotypic $KCu_2(H_3O_2)(SO_4)_2$, we refer to the original description [16] for further details.

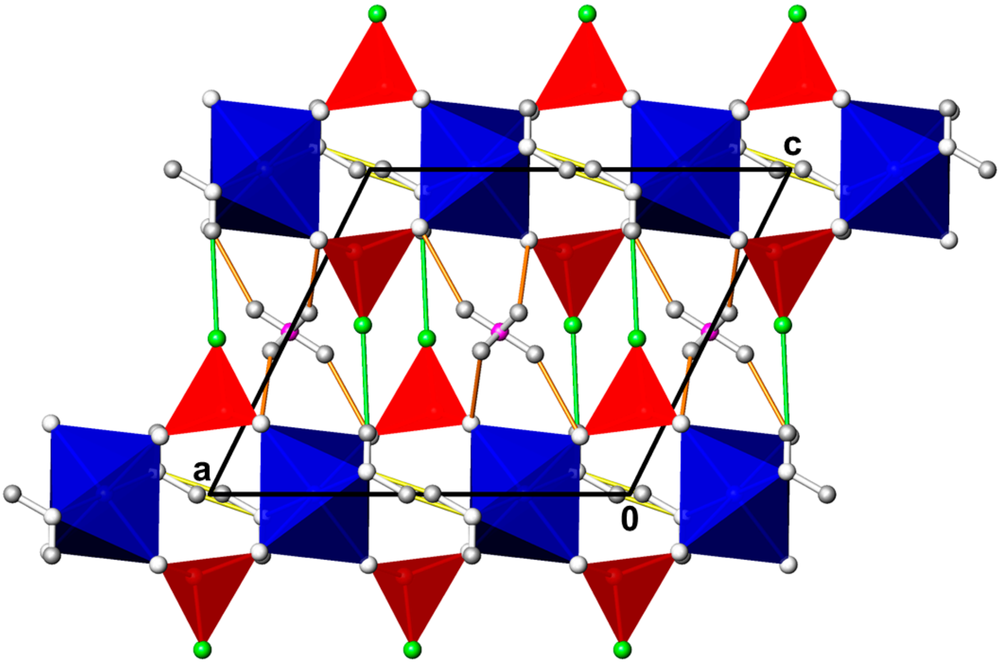

Figure 10. The crystal structure of $NH_4Cu_2(H_3O_2)(PO_3F)_2$ in a projection along [010]. Colour code as in Figure 6.

3.10. $(NH_4)_2Zn(PO_3F)_2(H_2O)_{0.2}$

Three ammonium cations, two zinc cations, three monofluorophosphate anions and one positionally and occupationally disordered water molecule are present in the asymmetric unit. Except one Zn site (Zn2) located on a twofold rotation axis (Wyckoff position 4*e*), all other atoms in this structure are located on general positions (Wyckoff position 8*f*). The O atoms of four monofluorophosphate anions tetrahedrally surround both zinc cations. The latter do not share common atoms but are bridged by the monofluorophosphate units into $(10\bar{1})$ layers. Within a layer disorder of the four O atoms around Zn2 over two sets of sites is observed, with atoms O4 and O8 having an occupational ratio of 0.65(3):0.35(3) for the split pair A:B. This disorder also affects the monofluorophosphate anions associated with P2 and P3 that share these O atoms with Zn2. Additionally, the water molecule (O1W) shows positional and occupational disorder. It is disordered over an inversion centre and shows an occupancy of 0.309(12); full occupation of this site would result in a value of 0.5, leading to a formula of $(NH_4)_2Zn(PO_3F)_2(H_2O)_{0.33}$. Neighbouring layers are linked through intermediate ammonium cations by medium to weak hydrogen bonds to the monofluorophosphate O atoms. The crystal structure of $(NH_4)_2Zn(PO_3F)_2(H_2O)_{0.2}$ is displayed in Figure 11.

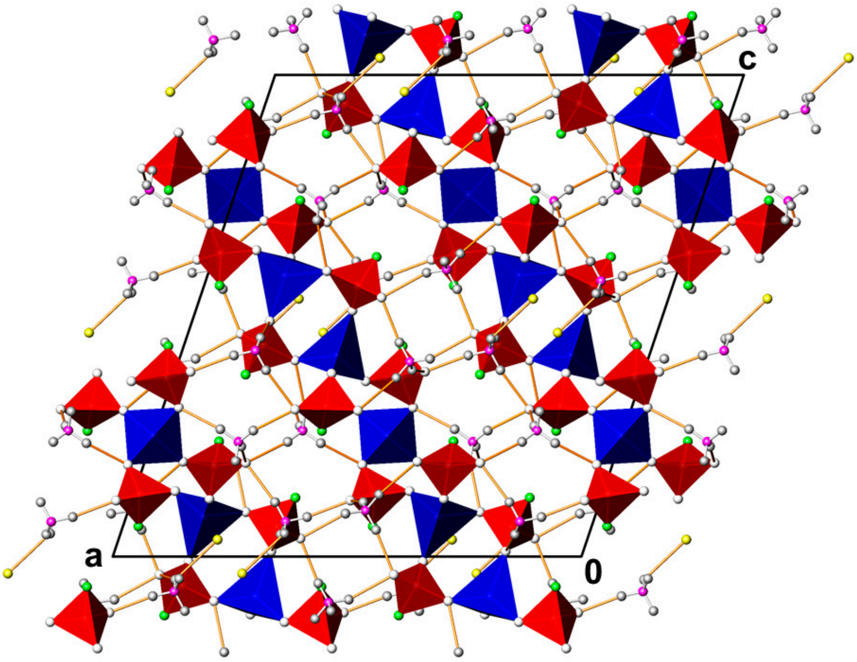

Figure 11. The crystal structure of $(NH_4)_2Zn(PO_3F)_2(H_2O)_{0.2}$ in a projection along [010]. Colour code of PO_3F tetrahedra and H atoms as in Figure 1; O atoms of disordered crystal water molecules are given as yellow spheres. For clarity, disorder involving parts of the $[ZnO_4]$ and PO_3F tetrahedra is not shown.

3.11. $(NH_4)_2Zn_3(PO_3F)_4(H_2O)$

$(NH_4)_2Zn_3(PO_3F)_4(H_2O)$ has a higher Zn and PO_3F content than $(NH_4)_2Zn(PO_3F)_2(H_2O)_{0.2}$ (ratio NH_4:Zn:PO_3F = 2:3:4 versus 2:1:2) but together with $ZnPO_3F(H_2O)_{2.5}$ also crystallized from the same solution. A very similar *I*-centred cubic unit cell (without further assignments of possible space groups) was reported for anhydrous $(NH_4)_2Zn_3(PO_3F)_4$ at room temperature (PDF entry #00-044-0539; a = 11.4769(5) Å). In the crystal structure of $(NH_4)_2Zn_3(PO_3F)_4(H_2O)$ disorder is observed, affecting the zinc and the ammonium sites. The major part of the cation (ZnA; occupancy 0.75) is situated on Wyckoff position 12*b* with $\bar{4}$ site symmetry. Due to disorder around this axis, the remaining Zn cations split into four equivalent sites (ZnB) with an occupancy of 0.0625 each. The N atom of the ammonium cation (N1H) and the O atom of a water molecule (O1W) simultaneously occupy Wyckoff position 12*a* (located on a $\bar{4}$ axis) in a ratio of 0.67:0.33. The site symmetry of the PO_3F tetrahedron is .3 with the P atom situated on Wyckoff position 16*c*. The disordered part of the crystal structure is shown in Figure 12.

Whereas ZnA is exclusively bonded to four O atoms (O1) of symmetry-related monofluorophosphate anions with an equal bond length of 1.934(3) Å, ZnB is coordinated by only three monofluorophosphate O atoms at two shorter and one longer Zn–O distances. The fourth coordination site, completing a distorted tetrahedron, is occupied by the water molecule at the longest distance of 2.204(14) Å. Again, the F atom of the monofluorophosphate tetrahedron does not take part in constructing the framework structure because it is not part of the coordination spheres around the two zinc sites (Figure 13). However, it is involved in weak hydrogen bonding interactions as the acceptor atom with the disordered (N1H/O1W) donor group. Two more hydrogen bonding interactions of similar strength are present between the donor group and the monofluorophosphate O atoms.

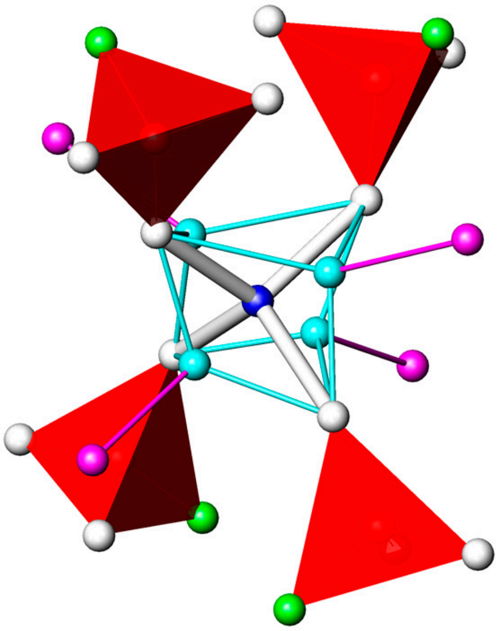

Figure 12. Disorder in the crystal structure of $(NH_4)_2Zn_3(PO_3F)_4(H_2O)$. Colour code of the PO_3F tetrahedra as in Figure 1. The major part of the disordered Zn site (ZnA) is given as a blue sphere, the minor part (ZnB) as a turquoise sphere. The statistically occupied (NH_4/H_2O) site is given in magenta. For clarity, H atoms are not shown.

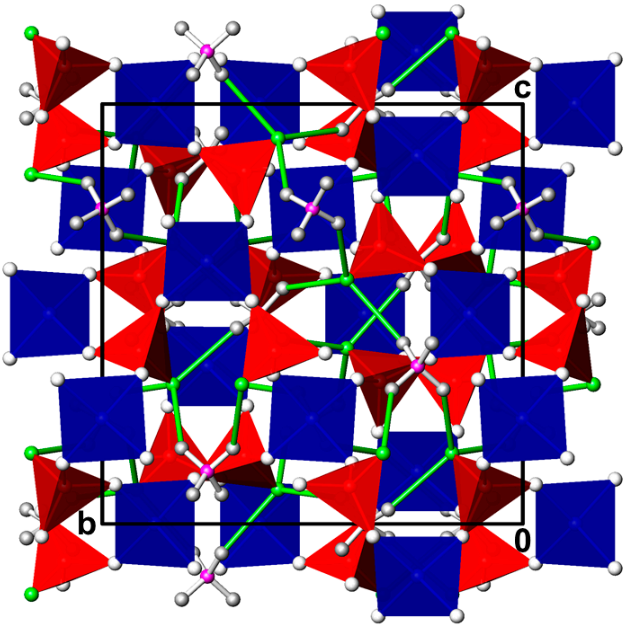

Figure 13. The crystal structure of $(NH_4)_2Zn_3(PO_3F)_4(H_2O)$ in a projection along $[\bar{1}00]$ giving only the major part of the disordered Zn site. Colour code of PO_3F tetrahedra as in Figure 1; $[ZnO_4]$ tetrahedra are given in blue and (N,O)–H···F hydrogen bonding is indicated by green lines. For clarity, (N,O)–H···O hydrogen bonding is not shown.

3.12. *Survey on the PO_3F^{2-} Group*

- **Mean bond lengths and angles in the PO_3F tetrahedron**

For the statistical analysis of bond lengths and angles within a PO_3F tetrahedron in inorganic monofluorophosphates that are compiled in the most recent version of the Inorganic Structure Database (ICSD, [31]), reliability factors $R1 \leq 0.08$ for the structure model and only ordered PO_3F groups were considered as criteria, disregarding different measurement temperatures or redeterminations. HPO_3F^- tetrahedra present in hydrogen-monofluorophosphates were not taken into account. In summary, 88 independent PO_3F tetrahedra from 63 different monofluorophosphate phases (including the examples of the current study) were used (Table 5). As a result, the P–F bond of 1.578(20) Å is significantly longer than the three P—O bonds with 1.506(13) Å, and relative to the ideal tetrahedral angle of 109.47°, the three O–P–O angles of 113.7(1.7)° are enlarged by about 4° and the O—P—F angle of 104.8(1.7)° reduced by about the same value. The averaged values for bond lengths and angles in the monofluorophosphate PO_3F tetrahedron differ markedly from those of the difluorophosphate PO_2F_2 tetrahedron. Here, the two P–O and the two P–F bonds are shortened with mean values of 1.459 (27) and 1.530 (21) Å, respectively, and the O–P–O angle once more is widened to 121.2 (2.9)°, whereas the O—P—F angle of 108.7 (6)° now is closer to the ideal value (the F–P–F angle is the smallest in the PO_2F_2 tetrahedron with 98.5 (2.6)°) [32]).

The computed mean values of the monofluorophosphate tetrahedron can be used as a simple tool for evaluation of crystal structures with this entity. In one case (Table 5), a significant deviation in terms of bond lengths and angles was observed for the crystal structure of $(NH_4)_3Fe(PO_3F)_2F_2$ [33] where one of the two distinct monofluorophosphate anions has one of the P–O bonds as the longest in the tetrahedron, a very short P–F bond, and with O–P–O and O–P–F angles unexpected: P2–O1 = 1.562(5) Å, P2–F4 = 1.498(5) Å, P2–O4 = 1.485(6) Å (2x); O1–P2–F4 = 106.7(3)°, O1–P2–O4 = 102.7(2)° (2x), F4–P2–O4 = 115.0(2)° (2x), O4–P2–O4 = 112.8(3)°. Based on the current averaged data for a PO_3F tetrahedron, it is clear that atoms O1 and F4 were wrongly assigned and must be interchanged.

- **Symmetry of the PO_3F group in crystal structures**

Possible point group symmetries of a PO_3F group in a crystal structure are 1, 3, *m* and 3*m*, the latter being the highest possible point group symmetry for this tetrahedron in the crystalline state. The vast majority of monofluorophosphate groups exhibits point group symmetry 1 (70 examples), followed by point group symmetry *m* (15 examples), 3*m* (two examples) and 3 (one example). The reported point group symmetry of $\bar{4}2m$ for the PO_3F group in $K_3(PO_3F)F$ [34] is incompatible with its molecular symmetry and consequently, this group is disordered.

- **Isotypism with sulfates**

From the numerous phases compiled in Table 5, only nine show isotypism with the corresponding sulfate, *viz.* $Na_2PO_3F(H_2O)_{10}$, $NaK_3(PO_3F)_2$, $K_3(PO_3F)F$, M_2PO_3F (M = K, Rb, Cs, NH_4), $(NH_4)_2Ni(PO_3F)(H_2O)_6$ and $CuK(OH)(PO_3F)(H_2O)$. Eleven monofluorophosphate phases have equivalent sulfate phases but with different crystal structures, *viz.* $Li(NH_4)PO_3F$, Na_2PO_3F, $CaPO_3F(H_2O)_2$, $SrPO_3F$, $BaPO_3F$, $(NH_4)Mn(PO_3F)F_2$, $Fe_2(PO_3F)_3$, $NaFe(PO_3F)_2$, $SnPO_3F$, Ag_2PO_3F, and Hg_2PO_3F, but the majority of monofluorophosphate phases has no sulfate counterpart.

- **Hydrogen bonding with the monofluorophosphate F atom as an acceptor**

As discussed briefly for appropriate structures above and detailed in Table 3, hydrogen bonding involving the F atom of the monofluorophosphate anion occurs only occasionally and then only as a comparatively weak interaction. A review of the crystal structures where hydrogen bonding is possible and where all H atoms were determined revealed that this situation holds also for most other monofluorophosphates. Considering a $D\cdots F$ distance (D = donor atom: N, O) less than 3.2 Å and D–H$\cdots$F angles greater than 130°, as relevant for a significant hydrogen bonding interaction [35], then only for $Li(NH_4)PO_3F$, $Na_2PO_3F(H_2O)_{10}$, $CaPO_3F(H_2O)_2$, $Cu_2K(OH)(H_2O)(PO_3F)_2$, $K_2Mn_3(HPO_4)_2(PO_3F)F$, and $(NH_4)_2Ni(PO_3F)_2(H_2O)_6$ is this kind of interaction realized, albeit of weak nature (Table 5). In all other monofluorophosphates capaple of hydrogen-bonding interactions either the $D\cdots$F–P distances are much greater than the threshold of 3.2 Å, or the D–H$\cdots$F angles are much smaller than 140°. In these structures, D–H$\cdots$O hydrogen bonds dominate or are the only hydrogen-bonding interactions.

Table 5. Structural details of monofluorophosphates, site symmetries of corresponding PO_3F tetrahedra, relation to the sulfate analogues and details of D–H···P–F hydrogen bonding.

Monofluorophosphate (Reference)	Space Group, Z	Site Symmetry PO_3F Group(s)	D–H···F–P Hydrogen Bonding with D···F/Å and D–H···F/°	Corresponding Sulfate	Relationship	Remark
$LiKPO_3F(H_2O)$ [36]	$P2_1/c$, 4	1	3.15; 120	-	-	-
$Li(NH_4)PO_3F$ [37]	$P2_1/c$, 4	1	2.98; 147	$Li(NH_4)(SO_4)$ $P2_1cn$, $Z = 4$; $P2_1/c$ $Z = 8$; $Pmcn$, $Z = 8$.	-	Sulfate shows poly-morphism.
Na_2PO_3F [38]	$P2_12_12_1$, 8	1, 1	-	Na_2SO_4 $Fddd$, $Z = 8$; $P6_3/mmc$, $Z = 2$.	-	Sulfate shows dimorphism.
$Na_2PO_3F(H_2O)_{10}$ [39]	$P2_1/c$, 4	1	2.83, 149 3.01, 178	$Na_2SO_4(H_2O)_{10}$ (Glauber salt)	Isotypic	-
$NaK_3(PO_3F)_2$ [40]	$P\bar{3}m1$, 1	$3m$	-	$NaK_3(SO_4)_2$ (glaserite)	Isotypic	-
$(NH_4)Na(PO_3F)(H_2O)$ [41]	Pn, 2	1	-	-	-	-
K_2PO_3F [6,42]	$Pnam$, 4	m	-	K_2SO_4 (arcanite); high-temperature form: $P6_3/mmc$; $Z = 2$.	Isotypic	Isotypic with low-temperature form;
$K_3(PO_3F)F$ [34]	$I4/mcm$, 4	$\bar{4}2m$	-	$K_3(PO_3F)F$	Isotypic,	PO_3F disordered. Phase transition reported for the sulfate.
Rb_2PO_3F [43]	$Pnma$, 4	m	-	Rb_2SO_4	Isotypic	K_2SO_4 structure type.
Cs_2PO_3F [43]	$Pnma$, 4	m	-	Cs_2SO_4	Isotypic	K_2SO_4 structure type.
$Cs_3(NH_4)_2(HPO_3F)_3(PO_3F)$ [44]	$P2_1/c$, 8	1,1,1,1	-	-	-	-
$(NH_4)_2(PO_3F)$ [45]	$Pna2_1$, 4	1	-	$(NH_4)_2(SO_4)$	Isotypic	Ferroelectric phase; K_2SO_4 structutre type.
$(NH_4)_2(PO_3F)(H_2O)$ [46–48]	$P2_1/c$, 4	1	-	-	-	-
$(NH_4)_2Mg(PO_3F)_2(H_2O)_2$ [this work]	$C2/m$, 2	m	-	-	-	-
$CaPO_3F(H_2O)_2$ [46]	$P\bar{1}$, 2	1	3.12, 147	$CaPO_4(H_2O)_2$ (gypsum) $C2/m$, $Z = 4$.	-	-
$SrPO_3F$ [49]	$P2_1/c$, 4	1	-	Barite-type $SrSO_4$; $Pnma$, $Z = 4$;	-	$SrPO_3F$ adopts the monazite structure type.
$SrPO_3F(H_2O)$ [49]	$P2_1/c$, 4	1	2.77, 108 2.95, 110	-	-	X-ray powder data.
$BaPO_3F$ [50]	$P2_1/c$, 8	1, 1	-	$BaSO_4$ (barite), $Pnma$, $Z = 4$; $F\bar{4}3m$, $Z = 4$ (HT)	-	Sulfate shows dimorphism.
$CsTi_2F_2(PO_4)(PO_3F)_2$ [51]	$P2/c$, 2	1	-	-	-	
$Cr_2(PO_3F)_3(H_2O)_{18.8}$ [this work]	$P\bar{1}$, 4	1, 1, 1, 1, 1, 1	?	-	-	H atoms not determined.
$NH_4Cr(PO_3F)_2(H_2O)_6$ [this work]	$R\bar{3}m$, 3	$3m$	-	-	-	-
$MnPO_3F(H_2O)_2$ [52]	$P\bar{1}$, 2	1	2.91, 111 3.11, 128 3.18, 127	-	-	-
$Li_3Mn(PO_3F)_2F_2$ [53]	$P2_1/c$, 2	1	-	-	-	-
$KMnF_2(PO_3F)$ [53]	$P2_1/n$, 4	1	-	-	-	-
$K_2Mn_3(HPO_4)_2(PO_3F)F$ [54]	$P2_1/c$, 4	1	3.09, 142 2.93, 122	-	-	-

Table 5. *Cont.*

Monofluorophosphate (Reference)	Space Group, Z	Site Symmetry PO_3F Group(s)	D–H···F–P Hydrogen Bonding with D···F/Å and D–H···F/°	Corresponding Sulfate	Relationship	Remark
$Rb_3Mn_3(PO_4)(PO_3F)_2F_5$ [53]	Cc, 4	1, 1	-	-	-	-
$Cs_2Mn_2F_4(PO_3F)_2$ [53]	$P2_1$, 2	1, 1	-	-	-	-
$(NH_4)_2Mn(PO_3F)_2(H_2O)_2$ [this work]	$P2_1/n$, 2	1	-	-	-	-
$(NH_4)Mn(PO_3F)F_2$ [53,55]	$P2_1/n$, 4	1	-	$NH_4Mn(SO_4)F_2$, $Pnna$, $Z = 8$.	-	-
$(NH_4)_2Mn_3(HPO_4)_2(PO_3F)F_2$ [54]	$P2_1/c$, 4	1	N–H 3.11, 160 O–H 2.87, 104	-	-	-
$(NH_4)Mn_3(PO_3F)_2(H_2PO_4)F_2$ [54]	$C2/c$, 4	1	O–H 2.97, 128	-	-	Same unit cell as $(NH_4)Mn_3(PO_3F)_2(PO_2F_2)F_2$ *.
$(NH_4)Mn_3(PO_3F)_2(PO_2F_2)F_2$ [56]	$C2/c$, 4	1	-	-	-	Same unit cell as $(NH_4)Mn_3(PO_3F)_2(H_2PO_4)F_2$ *.
$Ba_2Mn_2(PO_3F)F_6$ [57]	$P2_1/c$, 4	1	-	-	-	-
$Fe_2(PO_3F)_3$ [33]	$P6_3/m$, 6	m, m, m	-	$Fe_2(SO_4)_3$, $P2_1/n$, $Z = 4$; $R\bar{3}$, $Z = 6$.	-	Sulfate shows dimorphism.
$NaFe(PO_3F)_2$ [33]	$P2_1/c$, 4	1, 1	-	$NaFe(SO_4)_2$, $C2/m$, $Z = 2$	-	-
$KFe(PO_3F)F_2$ [54]	$P2_1/c$, 4	1	-	-	-	-
$KFe_2(PO_2F_2)(PO_3F)_2F_2$ [33]	$P\bar{1}$, 2	1, 1	-	-	-	-
$RbFe_3(PO_3F)((PO_2)_2(F_{1.5}(OH)_{0.5})_2)F_2$ [33]	$C2/c$, 4	1	-	-	-	-
$Cs_2Fe_2F_3(PO_3F)_2(PO_2F_2)$ [33]	$Aea2$, 4	1	-	-	-	-
$(NH_4)_2Fe_2(PO_3F)_2FCl_2$ [33]	$Pca2_1$, 4	1, 1	-	-	-	
$(NH_4)_3Fe(PO_3F)_2F_2$ [33]	$P2_1/m$, 4	m, m	-	-	-	H atoms not determined. F and O wrongly assigned for P2.
$CoPO_3F(H_2O)_3$ [58]	$P\bar{1}$, 2	1	2.98, 118	-	-	-
$(NH_4)_2Co(PO_3F)_2(H_2O)_2$ [this work]	$C2/m$, 2	m	-	-	-	-
$(NH_4)Co_3(PO_3F)_2(PO_2F_2)F_2$ [56]	$C2/c$, 4	1	2.96, 115	-	-	-
$Ba_2Co_2(PO_3F)F_6$ [55]	$P2_1/c$, 4	1	-	-	-	-
$(NH_4)_2(Ni(H_2O)_6)(PO_3F)_2$ [15]	$P2_1/c$, 2	1	2.84, 176	$(NH_4)_2(Ni(H_2O)_6(SO_4)_2$	Isotypic	Picromerite structure type.
$(NH_4)_2(Ni(H_2O)_6)(PO_3F)_2$ [this work]	$P2_1/c$, 2	1	2.81, 179	$(NH_4)_2(Ni(H_2O)_6$ $(SO_4)_2$	Isotypic	-
$Ba_2Ni_2(PO_3F)F_6$ [57]	$P2_1/c$, 4	1	-	-	-	-
$CuPO_3F(H_2O)_2$ [59]	$P2_1/c$, 4	1	-	-	-	-
$Cu_2K(OH)(PO_3F)_2(H_2O)$ [30]	$C2/m$, 2	m	3.00, 174	$Cu_2K(H_3O_2)$ $(SO_4)_2$	Isotypic	
$KCu_3(PO_2F_2)(PO_3F)_2F_2$ [55]	$C2/c$, 4	1	-	-	-	-
$RbCu_3(PO_2F_2)(PO_3F)_2F_2$ [55]	$C2/c$, 4	1	-	-	-	-
$NH_4Cu_2(H_3O_2)(PO_3F)_2$ [this work]	$C2/m$. 2	m	O–H 3.18, 177 N–H 2.97, 139	-$KCu_2(H_3O_2)(SO_4)_2$		Natrochalcite structure type.
$(NH_4)_2(Cu(H_2O)_2(PO_3F)_2)$ [27]	$C2/m$, 2	m	-	-	-	-
$Ba_2Cu_2(PO_3F)F_6$ [57]	$P2_1/c$, 4	1	-	-	-	

Table 5. *Cont.*

Monofluorophosphate (Reference)	Space Group, *Z*	Site Symmetry PO_3F Group(s)	*D*–H···F–P Hydrogen Bonding with *D*···F/Å and *D*–H···F/°	Corresponding Sulfate	Relationship	Remark
$ZnPO_3F(H_2O)_{2.5}$ [14]	$P\bar{1}$, 4	1, 1	-	-		H atoms not reliably determined.
$ZnPO_3F(H_2O)_{2.5}$ [this work]	$P\bar{1}$, 4	1, 1	-	-	-	-
$(NH_4)_2Zn(PO_3F)_2(H_2O)_{0.2}$ [this work]	$C2/c$, 12	1, 1, 1	?	-	-	H atoms of water not determined.
$(NH_4)_2Zn_3(PO_3F)_4(H_2O)$ [this work]	$I\bar{4}3d$, 4	3	(N,O)– 3.17, 141	-		-
$SnPO_3F$ [60]	$P2_1/c$, 4	1	-	Barite-type $SnSO_4$,*Pnma*, Z = 4	-	-
Ag_2PO_3F [4]	$C2/c$, 8	1	-	Ag_2SO_4, *Fddd*, Z = 8; $P6_3/mmc$, Z = 2	-	Sulfate shows dimorphism.
$(NH_4)Ag_3(PO_3F)_2$ [61]	*I*2, 8	1, 1, 1, 1	?	-		H atoms not determined
$CdPO_3F(H_2O)_2$ [this work]	$P\bar{1}$, 2	1	3.14, 121 3.09, 118	-		-
Hg_2PO_3F [21]	*Ibam*, 8	*m*	-	Hg_2SO_4, $P2/c$, Z = 2	-	-
$Pb_2PO_3FCl_2(H_2O)$ [this work]	*Pnma*, 4	*m*	?	-		H atoms not determined.

* It is most unlikely that $(NH_4)Mn_3(PO_3F)_2(PO_2F_2)F_2$ and $(NH_4)Mn_3(PO_3F)_2(H_2PO_4)F_2$ crystallize in the same type of structure with virtually the same unit cell and the same space group symmetry and differ only in one of the anions, i.e., PO_2F_2- and $PO_2(OH)_2^-$. In all likelihood, one of the crystal structure models (and the respective composition) is incorrect. Based on the available data, an evaluation was, however, not possible.

4. Conclusions

Single crystals of twelve and partly unknown monofluorophosphate phases were grown from aqueous solutions. Crystal structure refinements of these compounds extend our knowledge about the PO_3F^{2-} anion. Based on the present crystal structure data and a complete literature search addressing monofluorophosphate structures of inorganic compounds, the following structural characteristics for the tetrahedral PO_3F group were obtained: The P—F bond has a mean value of 1.578(20) Å and is considerably longer than the mean of the three P—O bonds of 1.506(13) Å, and the mean O–P–O angles of 113.7(1.7)° are considerably larger than the mean O–P–F angle of 104.8(1.7)°. The point group symmetry of the "free" PO_3F group (C_{3v} in Schoenflies or $3m$ in Hermann–Maugin notation) is found with this symmetry in the solid state only in two examples. In most cases (70 examples) the point group symmetry is reduced to C_1 (1) followed by point group symmetry C_s (m) with 15 examples and C_3 (3) with one example. The monofluorophosphate F atom is characterized by its isolated state in the crystal structure. In the vast majority of cases, it is not part of the coordination sphere of the cation and/or is not engaged in hydrogen bonding as an acceptor atom. Only in exceptional cases are weak interactions realized, i.e., for large cations with high coordination numbers in form of long metal–F bonds or as hydrogen bonds with long donor···F distances between 2.8 and 3.2 Å.

Funding: This research received no external funding.

Institutional Review Board Statement: Not applicable.

Informed Consent Statement: Not applicable.

Data Availability Statement: The data presented in this study are available in The Cambridge Crystallographic Data Centre (CCDC) and can be obtained free of charge via www.ccdc.cam.ac.uk/structures.

Acknowledgments: The author thanks Enrique J. Baran (Consejo Nacional de Investigaciones Científicas y Técnicas de la República Argentina (CONICET) and the Universidad Nacional de La Plata, Argentina) for recording and interpreting the vibrational spectra of $CdPO_3F(H_2O)_2$, and Ekkehard Füglein (Netzsch GmbH, Selb, Germany) for recording the TG of $CdPO_3F(H_2O)_2$.

Conflicts of Interest: The author declares no conflict of interest.

References

1. Lange, W. Über die Monofluorphosphorsäure und die Ähnlichkeit ihrer Salze mit den Sulfaten. *Ber. Dtsch. Chem. Ges.* **1929**, *62B*, 793–801. [CrossRef]
2. Rea, J.R.; Kostiner, E. The crystal structure of manganese fluorophosphate, $Mn_2(PO_4)F$. *Acta Crystallogr.* **1972**, *B28*, 2525–2529. [CrossRef]
3. Jin, D.; Qiu, H.; Du, F.; Wei, Y.; Meng, X. Co-doped Na_2FePO_4F fluorophosphates as a promising cathode material for rechargeable sodium-ion batteries. *Solid State Sci.* **2019**, *93*, 62–69. [CrossRef]
4. Weil, M.; Puchberger, M.; Füglein, E.; Baran, E.J.; Vannahme, J.; Jakobsen, H.J.; Skibsted, J. Single-Crystal Growth and Characterization of Disilver(I) Monofluorophosphate(V), Ag_2PO_3F: Crystal Structure, Thermal Behavior, Vibrational Spectroscopy, and Solid-State ^{19}F, ^{31}P, and ^{109}Ag MAS NMR Spectroscopy. *Inorg. Chem.* **2007**, *46*, 801–808. [CrossRef]
5. Xiong, L.; Chen, J.; Lu, J.; Pan, C.-Y.; Wu, L.-M. Monofluorophosphates: A New Source of Deep-Ultraviolet Nonlinear Optical Materials. *Chem. Mater.* **2018**, *30*, 7823–7830. [CrossRef]
6. Robinson, M.T. The crystal structures of β-K_2SO_4 and β-K_2PO_3F. *J. Phys. Chem.* **1958**, *62*, 925–928. [CrossRef]
7. Rây, R.C. Isomorphism and Chemical Homology. *Nature* **1930**, *126*, 310–311. [CrossRef]
8. Lima-de-Faria, J.; Hellner, E.; Liebau, F.; Makovicky, E.; Parthé, E. Nomenclature of Inorganic Structure Types—Report of the International Union of Crystallography Commission on Crystallographic Nomenclature Subcommittee on the Nomenclature of Inorganic Structure Types. *Acta Crystallogr.* **1990**, *A46*, 1–11. [CrossRef]
9. Gates-Rector, S.D.; Blanton, T.N. The Powder Diffraction File: A Quality Materials Characterization Database. *Powder Diffr.* **2019**, *34*, 352–360. [CrossRef]
10. McCubbin, F.M.; Phillips, B.L.; Adcock, C.T.; Tait, K.T.; Steele, A.; Vaughn, J.S.; Fries, M.D.; Atudorei, V.; Vander Kaaden, K.E.; Hausrath, E.M. Discreditation of bobdownsite and the establishment of criteria for the identification of minerals with essential monofluorophosphate (PO_3F^{2-}). *Am. Mineral.* **2018**, *103*, 1319–1328. [CrossRef]

11. Schülke, U.; Kayser, R. Herstellung von Fluorophosphaten, Difluorophosphaten, Fluorophosphonaten und Fluorophosphiten in fluoridhaltigen Harnstoffschmelzen. *Z. Anorg. Allg. Chem.* **1991**, *600*, 221–226. [CrossRef]
12. Sheldrick, G.M. A short history of *SHELX*. *Acta Crystallogr.* **2008**, *64*, 112–122. [CrossRef]
13. Sheldrick, G.M. Crystal structure refinement with *SHELXL*. *Acta Crystallogr.* **2015**, *71*, 3–8.
14. Durand, J.; Larbot, A.; Cot, L.; Duprat, M.; Dabosi, F. Etude Structurale de $ZnPO_3F{\cdot}2.5H_2O$, Nouvel Inhibiteur de Corrosion. *Z. Anorg. Allg. Chem.* **1983**, *504*, 163–172. [CrossRef]
15. Berraho, M.; R'Kha, C.; Vegas, A.; Rafiq, M. Structure of $Ni(H_2O)_6(NH_4)_2(PO_3F)_2$. *Acta Crystallogr.* **1992**, *C48*, 1350–1352. [CrossRef]
16. Chevier, G.; Giester, G.; Jarosch, D.; Zemann, J. Neutron Diffraction Study of the Hydrogen-Bond System in $Cu_2K(H_3O_2)(SO_4)_2)$. *Acta Crystallogr.* **1990**, *C46*, 175–177. [CrossRef]
17. Ross, S.D. *Inorganic Infrared and Raman Spectra*; McGraw Hill: London, UK, 1972.
18. Müller, A.; Baran, E.J.; Carter, R.O. Vibrational spectra of oxo-, thio-, and selenometallates of transition elements in the solid state. *Struct. Bond.* **1976**, *26*, 81–139.
19. Fadini, A.; Schnepel, F.M. *Vibrational Spectroscopy: Methods and Applications*; Ellis Horwood: Chichester, UK, 1989.
20. Siebert, H. *Anwendungen der Schwingungsspektroskopie in derAnorganischen Chemie*; Springer: Berlin, Germany, 1966.
21. Weil, M.; Puchberger, M.; Baran, E.J. Preparation and characterization of dimercury(I) monofluorophosphate(V), Hg_2PO_3F: Crystal structure, thermal behavior, vibrational spectra, and solid state ^{31}P and ^{19}F NMR spectra. *Inorg. Chem.* **2004**, *43*, 8330–8335. [CrossRef]
22. Calvo, C.; Au, P.K.L. Crystal structure of $Cd_2P_2O_7$. *Can. J. Chem.* **1969**, *47*, 3409–3416. [CrossRef]
23. Menz, D.-H.; Kolditz, L. Synthese und thermisches Verhalten von $Mg(NH_4)_2(PO_3F)_2{\cdot}2H_2O$. *Z. Chem.* **1985**, *25*, 189–190. [CrossRef]
24. Menz, D.-H.; Kolditz, L.; Heide, K.; Kunert, C.; Mensing, C. Zur Thermischen Zersetzung von $SrPO_3F{\cdot}H_2O$. *Z. Anorg. Allg. Chem.* **1986**, *540*, 191–197. [CrossRef]
25. Nyburg, S.C.; Steed, J.W.; Aleksovska, S.; Petruševski, V.M. Structure of the alums. I. On the sulfate group disorder in the α-alums. *Acta Crystallogr.* **2000**, *B56*, 204–209. [CrossRef] [PubMed]
26. Gmelin Handbook of Inorganic Chemistry. *Cr-Chrom (Systemnummer 52)*; Springer-Verlag: Berlin/Heidelberg, Germany, 1962; Teil B; p. 306ff.
27. Berraho, M.; Vegas, A.; Martinez-Ripoll, M.; Rafiq, M. A copper monofluorophosphate, $Cu(H_2O)_2(NH_4)_2(PO_3F)_2$. *Acta Crystallogr.* **1994**, *C50*, 666–668. [CrossRef]
28. Müller, U. *Symmetry Relationships between Crystal Structures*; IUCr/Oxford Science Publications: Oxford, UK, 2013.
29. Weil, M. On the (non-)existence of Tutton salts with formula types $[M(H_2O)_6](ClO_4)_2(H_2O)_2$ and $Na_2M(SO_4)_2(H_2O)_6$ (M is a first-row transition metal). *Acta Crystallogr.* **2013**, *C69*, 990–994. [CrossRef]
30. Moewius, F.; Ziemer, B.; Reck, G.; Meisel, M.; Grunze, H. Darstellung und Kristallstruktur von Kalium-dikupferhydroxid-bis(monofluorophosphat)-Monohydrat $Cu_2K(OH)(PO_3F)_2{\cdot}H_2O$. *Z. Anorg. Allg. Chem.* **1987**, *547*, 75–82. [CrossRef]
31. Zagorac, D.; Müller, H.; Ruehl, S.; Zagorac, J.; Rehme, S. Recent developments in the Inorganic Crystal Structure Database: Theoretical crystal structure data and related features. *J Appl. Crystallogr.* **2019**, *52*, 918–925. [CrossRef]
32. Weil, M.; Fürst, M. Crystal structure of (1,4-diphenyl-4*H*-1,2,4-triazol-3-yl)phenylamine difluorophosphate, and a survey of the difluorophosphate anion ($PO_2F_2^-$). *Acta Crystallogr.* **2020**, *E76*, 1003–1006. [CrossRef]
33. Keates, A.C.; Armstrong, J.A.; Weller, M.T. Iron fluorophosphates. *Dalton Trans.* **2013**, *42*, 10715–10724. [CrossRef]
34. Skakle, J.M.S.; Fletcher, J.G.; West, A.R. The crystal structures of potassium oxyfluorides, K_3SeO_4F and $K_3PO_3F_2$. *An. Quim. Int. Ed.* **1996**, *92*, 358–361.
35. Steiner, T. The Hydrogen bond in the Solid State. *Angew. Chem. Int. Ed.* **2002**, *41*, 48–76. [CrossRef]
36. Galigne, J.L.; Durand, J.; le Cot, L. Etudes structurales de composes oxyfluores du P(V). I. Structure crystalline de $LiKPO_3FH_2$ O. *Acta Crystallogr.* **1974**, *B30*, 697–701. [CrossRef]
37. Durand, J.; le Cot, L.; Galigne, J.L. Etudes structurales de composes oxyfluores du P(V). V. Structure crystalline de $LiNH_4PO_3F$. *Acta Crystallogr.* **1978**, *B34*, 388–391. [CrossRef]
38. Durand, J.; le Cot, L.; Galigne, J.L. Etudes structurales de composes oxyfluores du P(V) II. Structure cristalline de Na_2PO_3F beta. *Acta Crystallogr.* **1974**, *B30*, 1565–1569. [CrossRef]
39. Prescott, H.A.; Troyanov, S.I.; Kemnitz, E. The synthesis and crystal structures of two new hydrated sodium monofluorophosphates: $NaHPO_3F{\cdot}2.5H_2O$ (I) and $Na_2PO_3F{\cdot}10H_2O$ (II). *J. Solid State Chem.* **2001**, *156*, 415–421. [CrossRef]
40. Durand, J.; Granier, W.; le Cot, L.; Galigne, J.L. Etudes structurales de composes oxyfluores du P(V). III. Structure crystalline de $NaK_3(PO_3F)_2$. *Acta Crystallogr.* **1975**, *B31*, 1533–1535. [CrossRef]
41. Fabry, J.; Dušek, M.; Krupkova, R. Ammonium sodium fluorotrioxophosphate monohydrate. *Acta Crystallogr.* **2007**, *E63*, i92–i94. [CrossRef]
42. Payen, J.; Durand, J.; le Cot, L.; Galigne, J.L. Etude structurale du monofluorophosphate de potassium K_2PO_3F. *Can. J. Chem.* **1979**, *57*, 886–889. [CrossRef]
43. Fabry, J.; Dušek, M.; Fejfarova, K.; Krupkova, R.; Vanek, P.; Cisarova, I. Dirubidum fluorotrioxophosphate, Rb_2PO_3F, at 290 and 130 K, and dicesium fluorotrioxophosphate, Cs_2PO_3F, at 240 and 100 K. *Acta Crystallogr.* **2006**, *C62*, i49–i52. [CrossRef]
44. Prescott, H.; Troyanov, S.; Kemnitz, E. The crystal structures of two hydrogen monofluorophosphates: $CsHPO_3F$ and $Cs_3(NH_4)_2(HPO_3F)_3(PO_3F)$. *Z. Kristallogr.* **2000**, *215*, 240–245. [CrossRef]

45. Krupkova, R.; Fabry, J.; Cisarova, I.; Vanek, P. Bis(ammonium) fluorophosphate at room temperature. *Acta Crystallogr.* **2002**, *C58*, i66–i68. [CrossRef]
46. Perloff, A. The crystal structures of hydrated calcium and ammonium monofluorophosphates: $CaPO_3(H_2O)_2$ and $(NH_4)_2PO_3F(H_2O)$. *Acta Crystallogr.* **1972**, *B28*, 2183–2191. [CrossRef]
47. Berndt, A.F.; Sylvester, J.M. The crystal structure of ammonium monofluorophosphate: $(NH_4)_2PO_3F(H_2O)$. *Acta Crystallogr.* **1972**, *B28*, 2191–2193. [CrossRef]
48. Durand, J.; Beys, L.; Hillaire, P.; Aleonard, S.; le Cot, L. Etude structurale de $(NH_4)_2PO_3F$, H_2O a 120 K par diffraction des rayons X et spectroscopie Raman entre 293 et 83 K. *Spectrochim. Acta* **1978**, *A34*, 123–127. [CrossRef]
49. Jantz, S.G.; van Wuellen, L.; Fischer, A.; Libowitzky, E.; Baran, E.J.; Weil, M.; Höppe, H.A. Syntheses, crystal structures, NMR spectroscopy, and vibrational spectroscopy of $Sr(PO_3F).H_2O$ and $Sr(PO_3F)$. *Eur. J. Inorg. Chem.* **2016**, *7*, 1121–1128. [CrossRef]
50. Stöger, B.; Weil, M.; Skibsted, J. The crystal structure of $BaPO_3F$ revisited—A combined X-ray diffraction and solid-state ^{19}F, ^{31}P MAS NMR study. *Dalton Trans.* **2013**, *42*, 11672–11682. [CrossRef]
51. Marshall, K.L.; Weller, M.T. Synthesis of titanium fluorophosphates and fluorosulfates from hexafluorotitanic acid. *Z. Anorg. Allg. Chem.* **2014**, *640*, 2766–2770. [CrossRef]
52. Weil, M.; Baran, E.J.; Kremer, R.K.; Libowitzky, E. Synthesis, crystal structure, and properties of $Mn(PO_3F)(H_2O)_2$. *Z. Anorg. Allg. Chem.* **2015**, *641*, 184–191. [CrossRef]
53. Armstrong, J.A.; Williams, E.R.; Weller, M.T. Manganese(III) fluorophosphate frameworks. *Dalton Trans.* **2013**, *42*, 2302–2308. [CrossRef]
54. Wang, G.; Valldor, M.; Dorn, K.V.; Wilk-Kozubek, M.; Smetana, V.; Mudring, A.-V. Ionothermal Synthesis Enables Access to 3D Open Framework Manganese Phosphates Containing Extra-Large 18-Ring Channels. *Chem. Mater.* **2019**, *31*, 7329–7339. [CrossRef]
55. Armstrong, J.A.; Williams, E.R.; Weller, M.T. Fluoride-rich, hydrofluorothermal routes to functional transition metal (Mn, Fe, Co, Cu) fluorophosphates. *J. Am. Chem. Soc.* **2011**, *133*, 8252–8263. [CrossRef]
56. Jiang, J.; Zhu, B.; Zhu, T.; Yang, H.; Jin, Y.; Lü, M. Open-framework ammonium transition metal fluorophosphates with a Kagomé lattice network: Synthesis, structure and magnetic properties. *Dalton Trans.* **2020**, *49*, 841–849. [CrossRef] [PubMed]
57. Zhu, B.; Jiang, J.; Zhu, T.; Yang, H.; Jin, Y.; Choi, K.-Y.; Lü, M. Transition-Metal Monofluorophosphate $Ba_2M_2(PO_3F)F_6$ (M = Mn, Co, and Ni): Varied One-Dimensional Transition-Metal Chains and Antiferromagnetism. *Inorg. Chem.* **2020**, *59*, 3794–3804. [CrossRef] [PubMed]
58. Durand, J.; le Cot, L.; Berraho, M.; Rafiq, M. Structure du monofluorophosphate de cobalt trihydrate. *Acta Crystallogr.* **1987**, *C43*, 611–613.
59. Zeibig, M.; Wallis, B.; Moewius, F.; Meisel, M. Darstellung und Kristallstruktur von Kupfer(II)-monofluorophosphat-Dihydrat $CuPO_3F{\cdot}2H_2O$. *Z. Anorg. Allg. Chem.* **1991**, *600*, 231–238. [CrossRef]
60. Berndt, A.F. The crystal structure of $SnPO_3F$. *Acta Crystallogr.* **1974**, *B30*, 529–530. [CrossRef]
61. Weil, M. $NH_4Ag_3(PO_3F)_2$, a layered monofluorophosphate(V) with seven different Ag sites. *Acta Crystallogr.* **2007**, *C63*, i31–i33.